molecules

MDPI

Review

Synthesis of Graphene-Based Nanocomposites for Environmental Remediation Applications: A Review

Rohit Goyat [1], Yajvinder Saharan [1], Joginder Singh [1,*], Ahmad Umar [2,3,*,†] and Sheikh Akbar [3]

[1] Department of Chemistry, Maharishi Markandeshwar (Deemed to Be University), Mullana, Ambala 133203, Haryana, India
[2] Department of Chemistry, College of Science and Arts, and Promising Centre for Sensors and Electronic Devices (PCSED), Najran University, Najran 11001, Saudi Arabia
[3] Department of Materials Science and Engineering, The Ohio State University, Columbus, OH 43210, USA
* Correspondence: joginderchem@mmumullana.org (J.S.); ahmadumar786@gmail.com (A.U.)
† Visiting Professor at the Department of Materials Science and Engineering, The Ohio State University, Columbus, OH 43210, USA.

Abstract: The term graphene was coined using the prefix "graph" taken from graphite and the suffix "-ene" for the C=C bond, by Boehm et al. in 1986. The synthesis of graphene can be done using various methods. The synthesized graphene was further oxidized to graphene oxide (GO) using different methods, to enhance its multitude of applications. Graphene oxide (GO) is the oxidized analogy of graphene, familiar as the only intermediate or precursor for obtaining the latter at a large scale. Graphene oxide has recently obtained enormous popularity in the energy, environment, sensor, and biomedical fields and has been handsomely exploited for water purification membranes. GO is a unique class of mechanically robust, ultrathin, high flux, high-selectivity, and fouling-resistant separation membranes that provide opportunities to advance water desalination technologies. The facile synthesis of GO membranes opens the doors for ideal next-generation membranes as cost-effective and sustainable alternative to long existing thin-film composite membranes for water purification applications. Many types of GO–metal oxide nanocomposites have been used to eradicate the problem of metal ions, halomethanes, other organic pollutants, and different colors from water bodies, making water fit for further use. Furthermore, to enhance the applications of GO/metal oxide nanocomposites, they were deposited on polymeric membranes for water purification due to their relatively low-cost, clear pore-forming mechanism and higher flexibility compared to inorganic membranes. Along with other applications, using these nanocomposites in the preparation of membranes not only resulted in excellent fouling resistance but also could be a possible solution to overcome the trade-off between water permeability and solute selectivity. Hence, a GO/metal oxide nanocomposite could improve overall performance, including antibacterial properties, strength, roughness, pore size, and the surface hydrophilicity of the membrane. In this review, we highlight the structure and synthesis of graphene, as well as graphene oxide, and its decoration with a polymeric membrane for further applications.

Keywords: graphene; synthesis process; polymeric membranes; environmental remediation; composites

Citation: Goyat, R.; Saharan, Y.; Singh, J.; Umar, A.; Akbar, S. Synthesis of Graphene-Based Nanocomposites for Environmental Remediation Applications: A Review. *Molecules* **2022**, *27*, 6433. https://doi.org/10.3390/molecules27196433

Academic Editor: Panyong Kuang

Received: 25 August 2022
Accepted: 23 September 2022
Published: 29 September 2022

1. Introduction

Graphene is a purified form of graphite that recently gained enormous popularity in the energy [1–3], environment [4–8], membranes [1,7], sensor [9–12], and biomedical fields [13–26]. It is a sp^2 hybridized, hexagonally arranged, chain of polycyclic aromatic hydrocarbon with a honeycomb crystal lattice [27]. It is the most recent element of carbon allotropes and is actually the basic building block of other important carbon allotropes, including 3D graphite, 1D carbon nanotubes (CNTs), and 0D fullerene (C60), as shown in Figure 1.

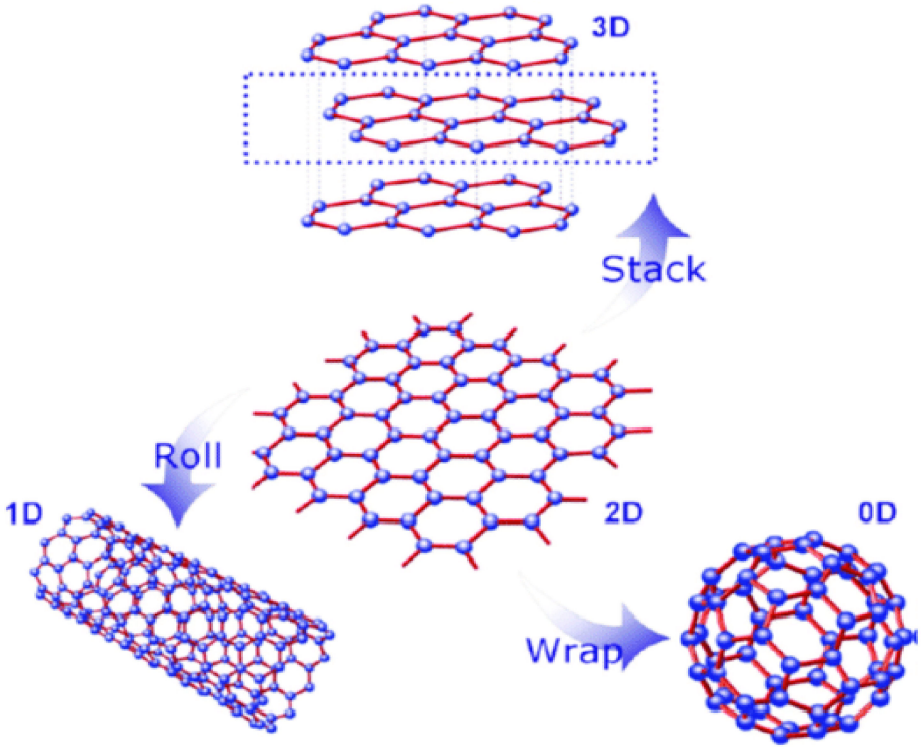

Figure 1. Structural representation of 2D graphene with different dimensions. [Reprinted with permission from ref. [28], Wan, X., Huang, Y., & Chen, Y. (2012). Focusing on energy and optoelectronic applications: a journey for graphene and graphene oxide at large scale. *Accounts of chemical research*, *45*(4), 598–607. Copyright © American Chemical Society].

The name graphene was coined by Boehm in 1986 [1], taking the prefix "graph" from graphite and the suffix "-ene" for sp^2 hybridized carbon, and was finally accepted by the International Union for Pure and Applied Chemistry in 1997 [29–33]. Furthermore, it became famous worldwide in 2004 when Geim and Novoselov obtained a single sheet of graphene on solid support, for which they were honored with the Nobel Prize in Physics in 2010 [34]. The main achievements of graphene in a timeline of history from 1840 to 2018 are shown in Figure 2.

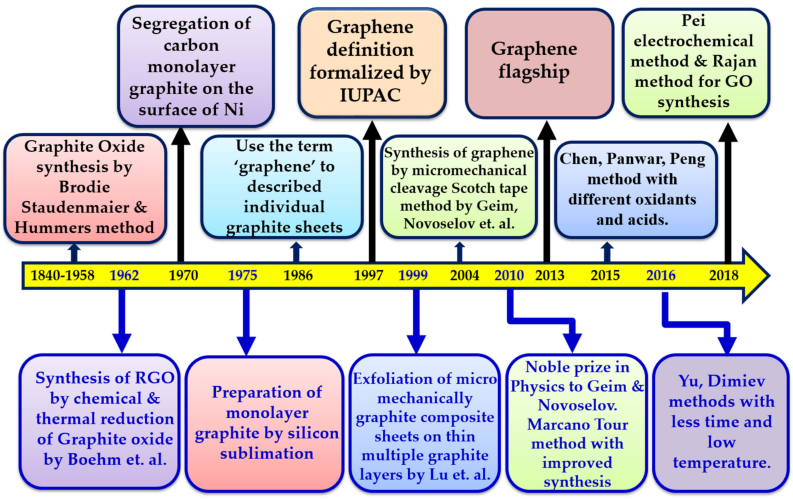

Figure 2. Schematic representation of a graphene timeline.

2. General Methods of Graphene Synthesis

Generally, graphene can be synthesized using two different routes, viz, bottom-up and top-down [33,35,36], as depicted in Figure 3.

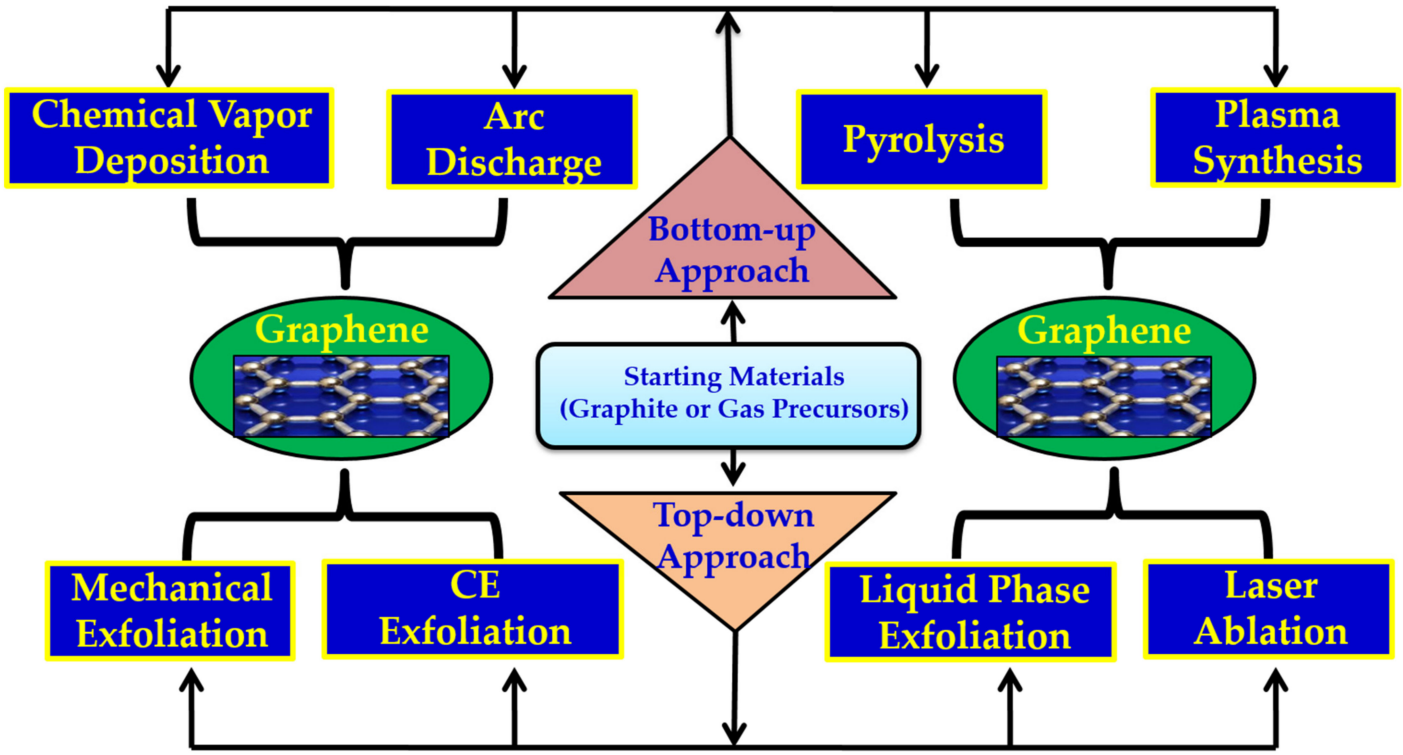

Figure 3. Schematic representation of the general methods for graphene synthesis.

2.1. Top-Down Method

In this method, graphite is exfoliated or converted into graphene [35,37] via mechanical, electrochemical exfoliation, laser ablation, and chemical/electrochemical fabrication.

2.1.1. Mechanical Exfoliation

This method involves the stripping/peeling of layers of graphite using adhesive tape onto a SiO_2 substrate. It was first invented by K. Novoselov and Andre Geim in 2004, and they were honored with a Nobel Prize for this invention [38]. Similarly, in 2017, Dasari et al. showed a micromechanical exfoliation of graphene sheets with adhesive Scotch tape [32]. Graphite was repeatedly peeled using adhesive tape until a single sheet of graphene was obtained, as depicted in Figure 4. Although this method is straightforward and is commonly used in laboratories, the obtained graphene has quite a low yield with few structural defects [38].

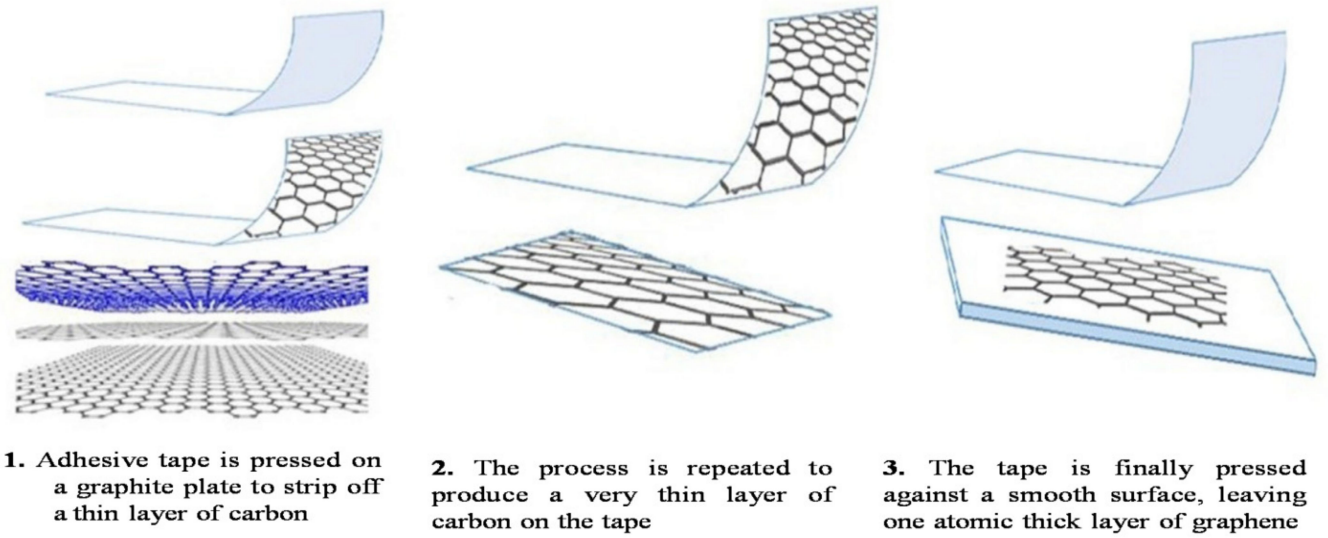

Figure 4. Mechanical exfoliation of graphene using the Scotch tape method [Reprinted with permission from ref. [39] Ibrahim, A.; Klopocinska, A.; Horvat, K.; Abdel Hamid, Z. Graphene-Based Nanocomposites: Synthesis, Mechanical Properties, and Characterizations. *Polymers* **2021**, *13*, 2869. https://doi.org/10.3390/polym13172869, Copyright © MDPI].

2.1.2. Electrochemical Exfoliation

Electrochemical exfoliation is a technique in which the graphite as an electrode is exfoliated in an electrochemical cell under the effect of different electrolytes to give pure graphene. When a current is applied to the electrochemical cell, up to three layer of graphene sheets are exfoliated from the graphite, along with the formation of graphene intercalation compounds [40,41]. Many researchers tried different electrolytes for the exfoliation of graphite, resulting in improvements in size, thickness, and the chemical and electronic properties of graphene.

In other attempts by Parvez et al. in 2013, an electrolytic cell was prepared using graphite as an anode and platinum or other metal as cathode. The electrodes were immersed in an electrolyte solution of sulfuric acid with potential of +10 V for 10 min. The yield of this process was more than 60%, and the obtained graphene had multiple layers [42]. Similarly, Liu et al., 2013 used pencil graphite for both electrodes with 1.0 M H_3PO_4 as an electrolyte, and the obtained graphene was not homogeneous, with defects in thickness and size distribution [43]. Hence, the electrochemical exfoliation of graphite has gained concern as an easy and eco-friendly method to synthesize good-quality graphene.

2.1.3. Liquid Phase Exfoliation

Liquid phase exfoliation (LPE) is another top-down method in which sonication is performed for the exfoliation of the graphite into graphene layers, as depicted in Figure 5. In 2008, Hernandez et al. and Lotya et al. in 2009, used LPE sonication with different solvents, viz, acetic acid, sulfuric acid, and hydrogen peroxide, resulting in graphite converted to graphene [44–46]. The time of sonication was typically 50–55 min with a power supply of 280–500 W. In 2008, Li et al. confirmed that nanoribbons of graphene were produced using an LPE method wherein the width was less than 10 nm.

Further in 2009, Green and Hersam used sodium cholate as a surfactant for the exfoliation of graphite [47]. The advantage of LPE is that it is a reliable, scalable method for the synthesis of graphene, but high energy consumption and low yield are the main challenges that need to be addressed.

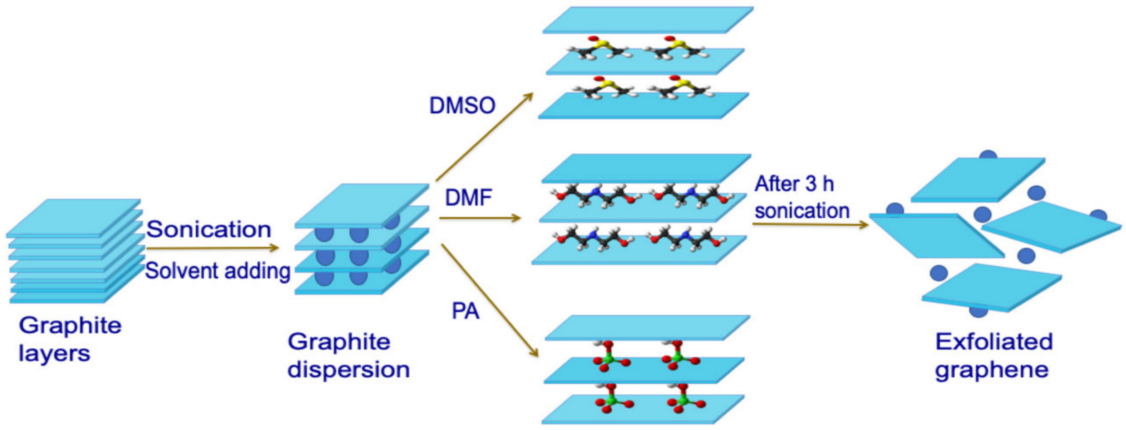

Figure 5. Schematic representation of the liquid phase exfoliation method [Reprinted with permission from ref. [48] Gürünlü, B.; Taşdelen-Yücedağ, Ç.; Bayramoğlu, M. Graphene Synthesis by Ultrasound Energy-Assisted Exfoliation of Graphite in Various Solvents. *Crystals* **2020**, *10*, 1037. https://doi.org/10.3390/cryst10111037, Copyright © MDPI].

2.1.4. Laser Ablation

In this technique, the laser erodes the carbon surface and produces graphene of the required quality. Several parameters, viz., laser beam repetition rate, wavelength, and pulse duration, must be checked during the synthesis process [49]. Secondly, the pressure of the gas in the background, the substrate distance, and the process temperature should also be in proper control [49–51]. Cappeli et al. opted for this technique in 2015 using silicon (Si) as a substrate [52]. He used a neodymium-doped yttrium aluminium garnet laser at different temperatures to obtain a high-quality graphene as shown in Figure 6. Further, in 2010 Koh et al. used ultra-short pulse laser technology with different substrates such as nickel, copper, cobalt, and iron for graphene synthesis [53]. The obtained graphene was of high quality with minimal size defects. Moreover, this process was quite eco-friendly with the ease of the experimental settings resulting in long-lasting graphene stability [54,55]. The noticeable disadvantages of this process were high energy inputs and the requirement for a much less laser-irradiating region for evaporating the target material.

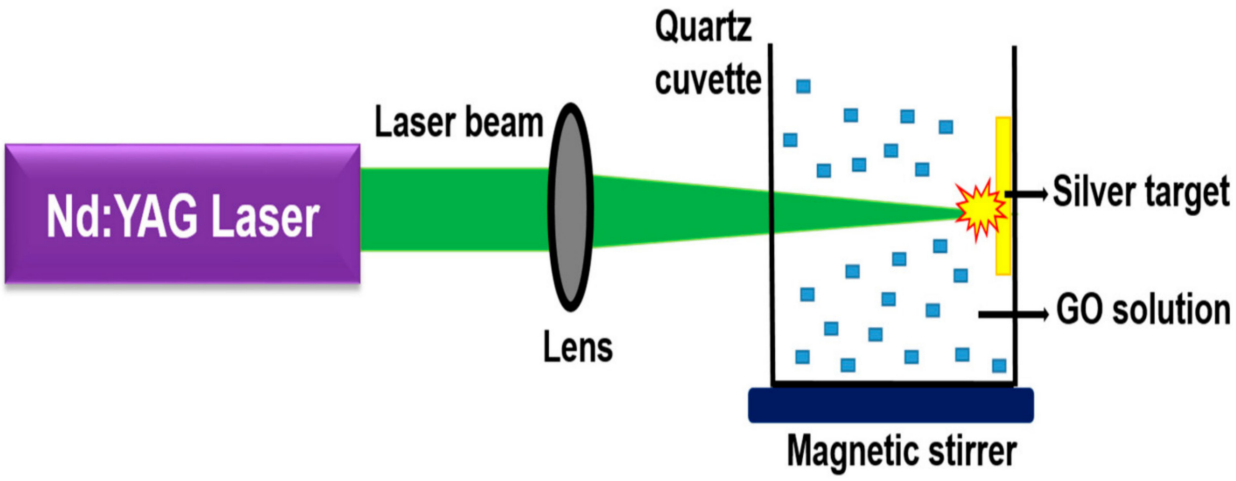

Figure 6. Schematic representation of the laser ablation method for graphene synthesis [Reprinted with permission from ref. [56] Nancy, P.; Jose, J.; Joy, N.; Valluvadasan, S.; Philip, R.; Antoine, R.; Thomas, S.; Kalarikkal, N. Fabrication of Silver-Decorated Graphene Oxide Nano-hybrids via Pulsed Laser Ablation with Excellent Antimicrobial and Optical Limiting Performance. *Nanomaterials* **2021**, *11*, 880. https://doi.org/10.3390/nano11040880, Copyright © MDPI].

2.2. Bottom-Up Method

This method is generally a self deposition or self-assembling process of nanoparticles carried out using four subtechniques, such as: arc discharge, chemical vapor deposition, pyrolysis, and plasma-enhanced chemical vapor deposition. In these subtechniques, the deposition of the graphite is carried out under controlled parameters like pressure, temperature, and flow rate [57]. The obtained graphene is of superior quality, having zero structural defects and possessing good electronic properties. However, the yield of the obtained graphene was rather low and could be used for limited applications.

2.2.1. Chemical Vapor Deposition (CVD)

In CVD, general equipment consists of tube furnace, gas flow, substrates, and tail gas treatment, as depicted in Figure 7. The commonly used substrates are from group B elements, which allow a low-energy pathway by forming intermediate compounds for the synthesis of graphene. The first row of d-block metals, viz, copper, cobalt, iron, and nickel, attracts huge interest due to their high availability and cost effectiveness [58]. The difference in the solubility of carbon with transition metals influences the growth quality of graphene [59]. Iron shows the highest carbon solubility, while copper has the lowest. For this reason, copper is a perfect metal to synthesize mono layer graphene, whereas, when both nickel and cobalt are used, multiple layers of graphene are often obtained. Graphene with a large surface area can be synthesized by exposing the precursors at extreme heat, wherein a copper or nickel substrate is placed at temperatures of 1000 °C in a reactor [60]. Furthermore, several scientists discussed the use of group B metals for the synthesis of graphene at large scale [60–65]. The quality of the substrate, temperature, and pressure provided on the surface of the substrate also regulates the synthesis of graphene in this process [66]. Due to the large number of interdependent parameters, the optimization process of the quality of graphene is typically very difficult in this process.

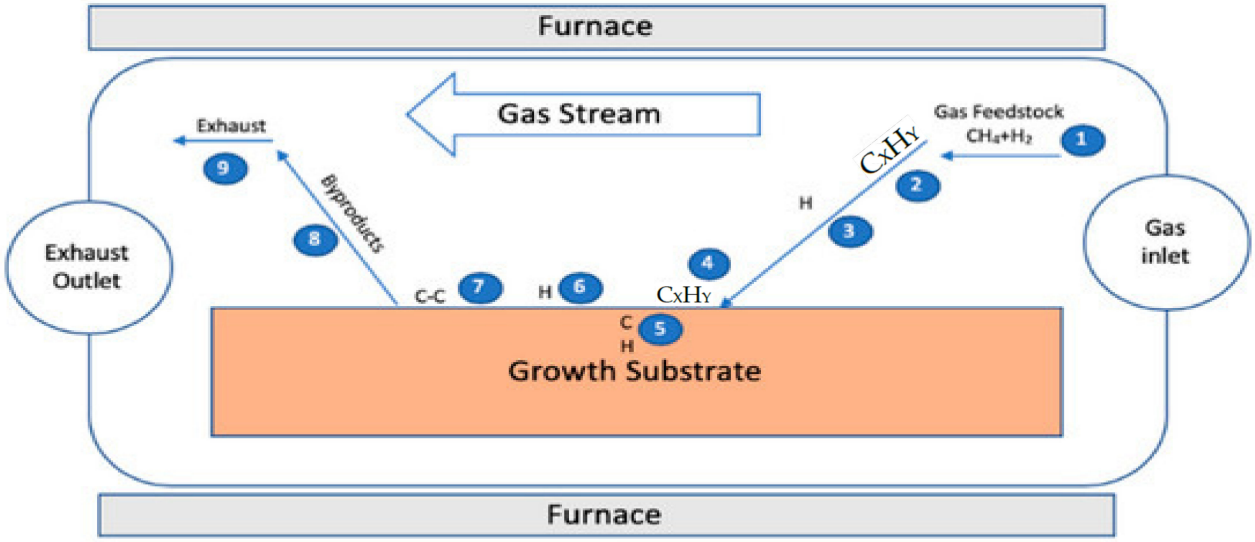

Figure 7. Schematic representation of the CVD method for graphene [Reprinted with permission from ref. [67], Saeed, M.; Alshammari, Y.; Majeed, S.A.; Al-Nasrallah, E. Chemical Vapour Deposition of Graphene Synthesis, Characterisation, and Applications: A Review. *Molecules* **2020**, *25*, 3856. https://doi.org/10.3390/molecules25173856, Copyright © MDPI].

2.2.2. Arc Discharge

Krastchmer and Hoffman were the first to use the arc discharge method. In this method, an electric arc oven comprises two graphite electrodes with a steel chamber cooled with water, and further direct current arc voltage is applied across these two graphite electrodes immersed in an inert gas, as shown in Figure 8. Wu et al. in 2010 proposed the

arc discharge method to synthesize graphene under the gaseous atmospheric conditions. He used a combination of hydrogen and nitrogen gases, to generate a graphene with good quality [68]. In comparison to chemical methods, the graphene produced had fewer structural defects and was easily dispersible in organic solvents, which enhanced its further applications. Other combination of gases, such as helium and carbon dioxide, were also tried, resulting in high-quality graphene production. Using the same process, the good quality bi- and tri-layers of graphene were reported in 2016 by Kim et al. [69]. In addition to this, in 2018, Cheng et al. combined vacuum arc discharge by using the CVD method for graphene synthesis [70]. Hence, arc discharge is an eco-friendly, cost-effective method that yields high-purity graphene.

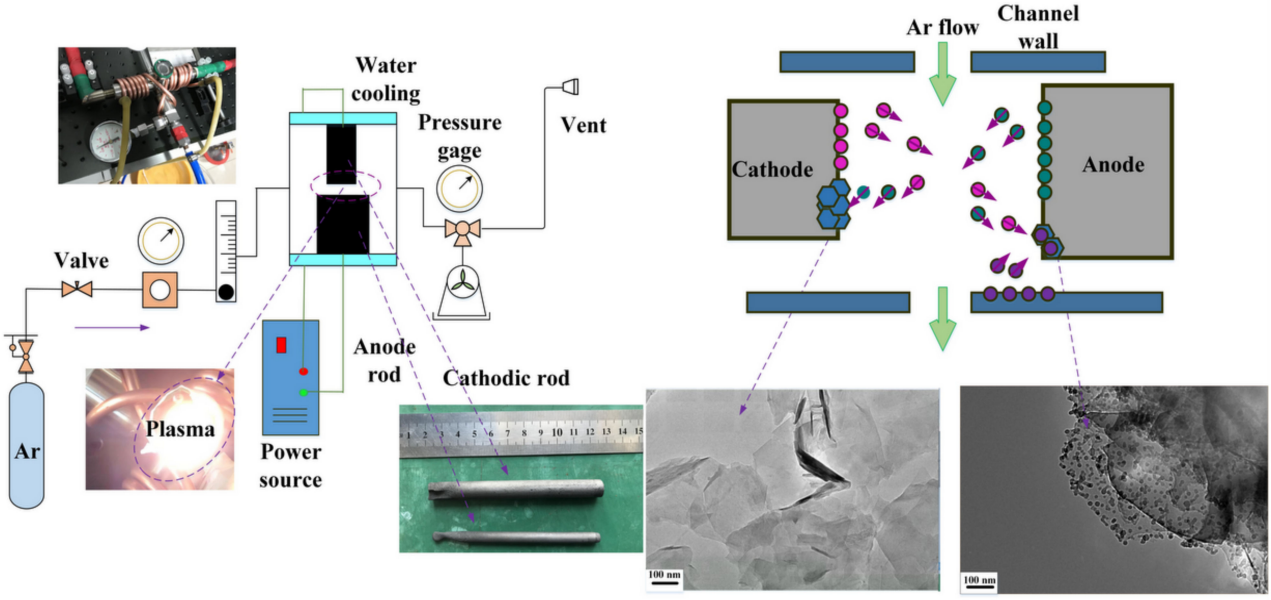

Figure 8. Schematic representation of the arc discharge method for the synthesis of graphene [Reprinted with permission from ref. [71], Tan, H.; Wang, D.; Guo, Y. A Strategy to Synthesize Multi-layer Graphene in Arc-Discharge Plasma in a Semi-Opened Environment. *Materials* **2019**, *12*, 2279. https://doi.org/10.3390/ma12142279, Copyright © MDPI].

2.2.3. Plasma-Enhanced Chemical Vapor Deposition Synthesis (PECVD)

The PECVD process is commonly designed to produce graphene from a hydrogen/methane gas mixture on copper and nickel samples. It is an additional method for the production of graphene that is similar to the thermal CVD process [71–76]. The process depends on the number of plasma sources, such as microwave (MW) [77], radio frequency [78], and direct current (dc) arc discharge [79]. Both copper and nickel are generally taken as the core substrates for PECVD graphene synthesis; yet, some other substrates have also been used [80,81]. The typical conditions for PECVD graphene synthesis on the metal substrate are methane in hydrogen (5–100%), with a substrate temperature in the range of 500 to 800 °C [81,82] and 900 W plasma power. The main advantage of this method is the low temperature and short time duration (<5 min) in comparison to thermal CVD.

2.2.4. Pyrolysis

The pyrolysis or devolatilization process is the thermal decomposition of materials at high temperature in the atmosphere of inert gases. A change occurs in the chemical onfiguration of the starting material. To fabricate few-layer graphene, carbon atoms were synthesized on a metal surface. One of the familiar techniques to synthesize graphene is the thermal decomposition of silicon carbide (SiC) [83]. At elevated temperature, Si is desorbed, leaving behind carbon. The obtained graphene sheets have thickness up to 10 μm. The major advantages of this scheme are that it is cost-effective, providing for the

simple fabrication of graphene. The advantages and disadvantages of the above-mentioned methods used for graphene synthesis are mentioned in Table 1 given below.

Table 1. Advantages and disadvantages of various methods used to synthesize graphene.

Top Down Method					
S. No	**Methods**	**Thickness of Graphene Obtained**	**Advantage**	**Disadvantage**	**Reference**
1	Micromechanical exfoliation	Single layer of graphene	Simple method with the formation of large size layers of graphene	Low yield	[32–38]
2	Electrochemical exfoliation	Single and few layers of graphene formed	High yield and quick process	Having structural defects and workup is expensive.	[40–43]
3	Liquid phase exfoliation	Mostly single layers of graphene obtained	Reliable and scalable method with the high exfoliation of graphite	Involves the use of hazardous chemical (chloro sulfonic acid) and the removal of used acid in the process is costly	[45–47]
4	Laser ablation	Single, bi, and multiple layers of graphene	Rapid, simple, and eco-friendly process with high-quality graphene.	Small laser-irradiating area for evaporating the target material	[49–55]
Bottom Up Method					
S. No	**Techniques**	**Thickness**	**Advantage**	**Disadvantage**	**Reference**
1	CVD	Mono and few-layer graphene sheets	Large size sheets of graphene obtained	Difficult to control numerous parameters	[61–66]
2	Arc discharge	Single, bi, and few layers of graphene	Cost-effective method with high-quality product	Requires a gaseous atmosphere, and the product contains structural defects	[68–70]
3	Plasma enhanced chemical vapor deposition	Bi and tri layers of graphene	Low temperature and less duration with high production	Requires high plasma power and different substrates	[74–81]
4	Pyrolysis	Few-layer graphene	Requires low cost and the high quality of graphene produced	Method used on a small scale	[83]

3. Graphene Oxide (GO)

In comparison to graphene, graphene oxide is considered a more versatile and advanced material. GO has a broad range of oxygen containing functional groups such as carboxyl, hydroxyl, epoxy, carbonyl, and keto groups on its surface, as shown in Figure 9 [84–87].

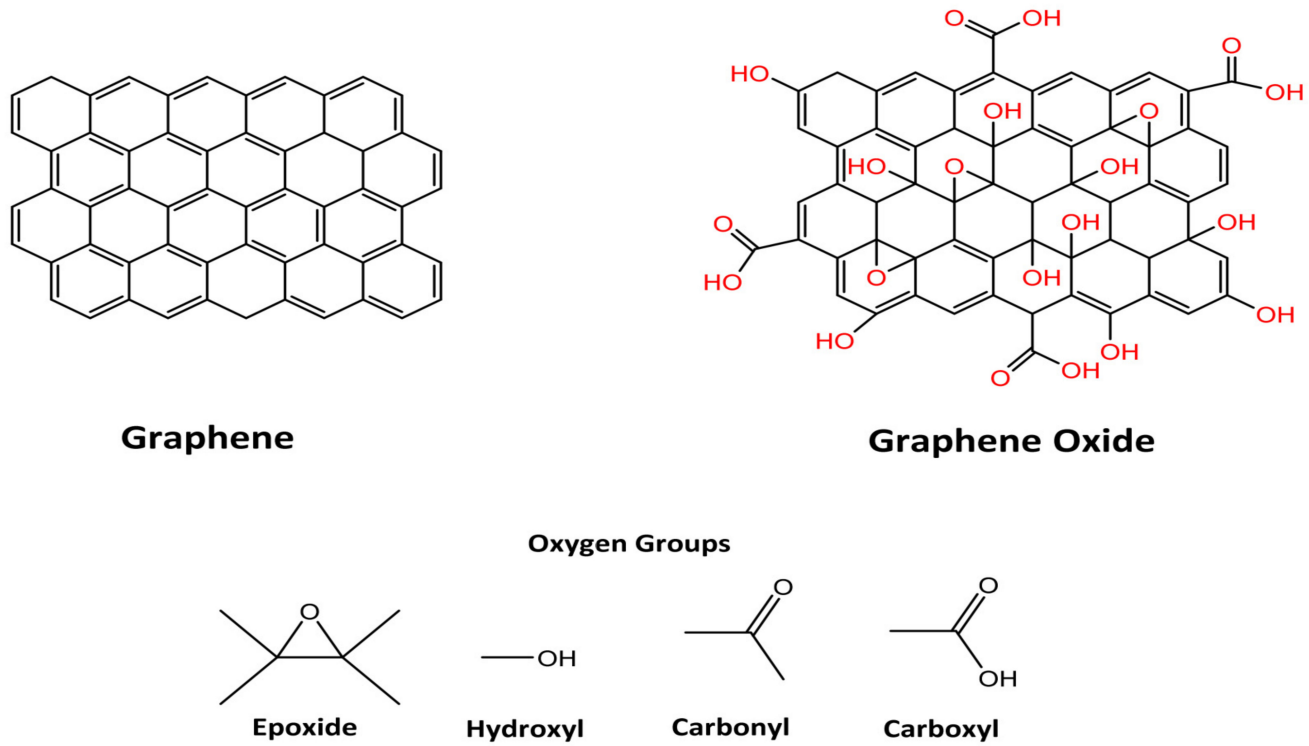

Figure 9. Schematic representation of the graphene and graphene oxide structures and graphene oxide oxygenated groups. [Reprinted with permission from ref. [87], Olean-Oliveira, A.; Oliveira Brito, G.A.; Cardoso, C.X.; Teixeira, M.F.S. Nanocomposite Materials Based on Electrochemically Synthesized Graphene Polymers: Molecular Architecture Strategies for Sensor Applications. *Chemosensors* **2021**, *9*, 149. https://doi.org/10.3390/chemosensors9060149, Copyright © MDPI].

GO has shown great potential in a variety of fields by virtue of its high surface area [88], unique mechanical strength [89], and excellent optical and magnetic properties [90]. In comparison to other carbon-based nanomaterials, GO is considered a green oxidant, as it is enriched with oxygen-containing functional groups [91,92]. Further, GO has an aromatic scaffold, which acts as a template to anchor active species behaving as an organo-catalyst [93,94]. Hence, GO can replace conventional materials in a variety of applications in different fields as shown in Figure 10.

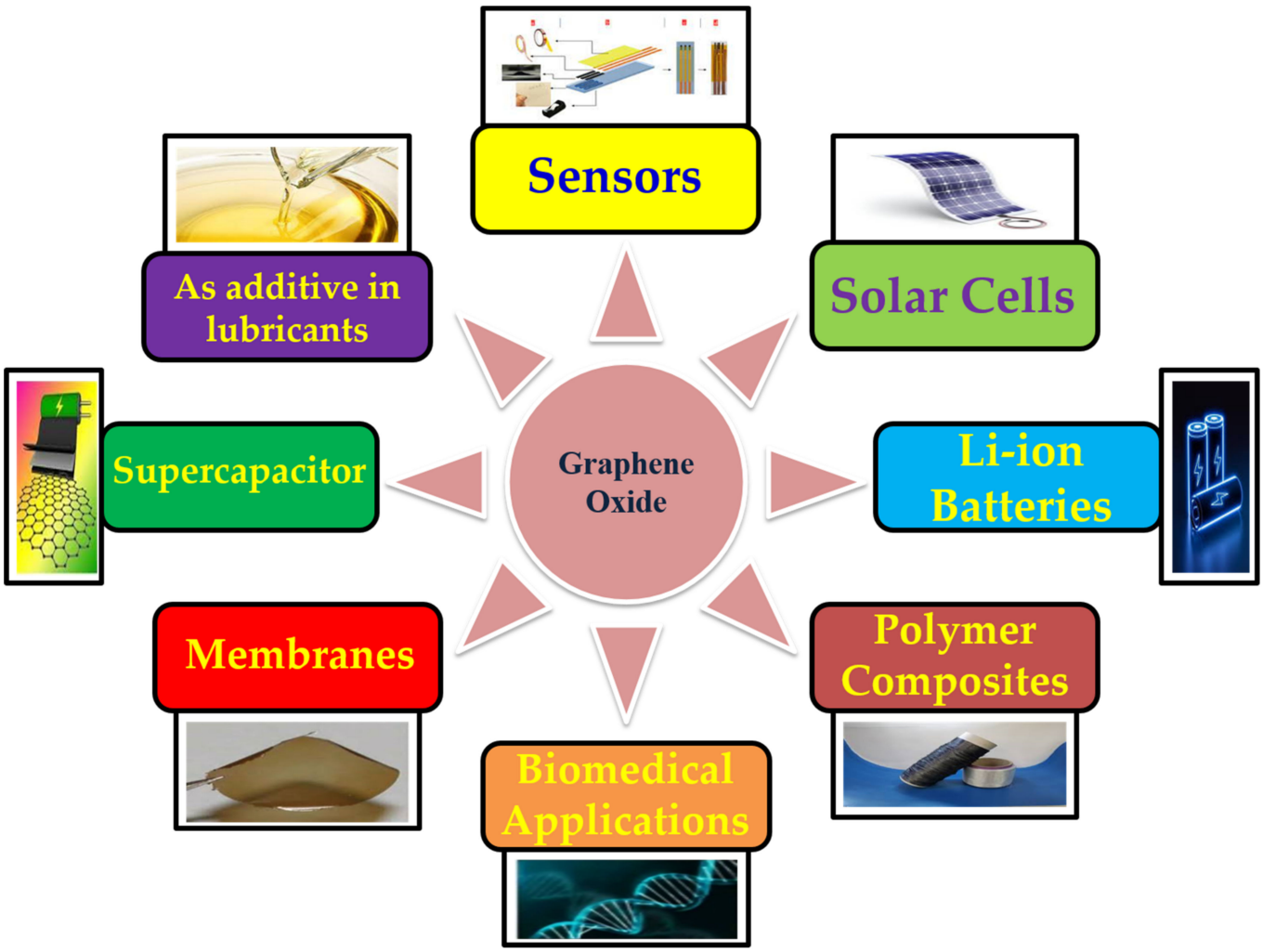

Figure 10. Schematic representation of the various applications of graphene oxide.

3.1. Synthesis of GO

In 1840, German scientist Schafhacutl was given the first report on the synthesis of graphene oxide and graphite intercalated compounds [95]. For the very first time, he attempted to exfoliate graphite and tried to purify impure graphite "kish" from iron smelters [27]. To date, several methods, as shown in Table 2, have been proposed.

Table 2. List of different methods used to synthesize graphene oxide.

Methods	Year	Starting Material	Different Oxidants Used	Reaction Time for GO Synthesis	Temperature °C	Features	References
Brodie	1859	Graphite	$KclO_3$, HNO_3	3–4 days	60	First attempt to synthesize GO	[96]
Staudenmaier	1898	Graphite	$KclO_3$, H_2SO_4, HNO_3	96 h	Room temperature	Improved efficiency	[97]
Hummers	1958	Graphite	$KmnO_4$, H_2SO_4, $NaNO_3$	<2 h	<20–35–98	Water-free, less than 2 h of reaction time	[98]
Fu	2005	Graphite	$KmnO_4$, H_2SO_4, $NaNO_3$	<2 h	35	Validation of $NaNO_3$	[99]
Shen	2009	Graphite	Benzoyl peroxide	10 min	110	Fast and non-acidic	[100]
Su	2009	Graphite	$KmnO_4$, H_2SO_4	4 h	Room temperature	Large-size GO sheets formed	[101]
Marcano and Tour	2010 & 2018	Graphite	$KmnO_4$, H_3PO_4, H_2SO_4	12 h	50	Eco-friendly resulting in a high yield	[102]
Sun	2013	Graphite	$KmnO_4$, H_2SO_4	1.5 h	Room temperature-90	High-yield and safe method	[103]
Eigler	2013	Graphite	$KmnO_4$, $NaNO_3$, H_2SO_4	16 h	10	High-quality GO produced	[104]
Chen	2015	Graphite	$KmnO_4$, H_2SO_4	<1 h	40–95	High-yield product	[105]
Panwar	2015	Graphite	H_2SO_4, H3PO4, $KmnO_4$, HNO_3	3 h	50	Three component acids and high-yield product	[106]
Peng	2015	Graphite	K_2FeO_4, H_2SO_4	1 h	Room temperature	Results in a high-yield and eco-friendly method	[107]
Rosillo-Lopez	2016	Graphite	HNO_3	20 h	Room temperature	Nano-sized GO obtained	[108]
Yu	2016	Graphite	K_2FeO_4, $KmnO_4$ H_2SO_4, H_3BO_3	5 h	<5–35–95	Low manganite impurities and high yield obtained	[109]
Dimiev	2016	Graphite	$(NH_4)_2S_2O_8$ 98% H_2SO_4, fuming H_2SO_4	3–4 h	Room temperature	25 nm thick and ~100%conversion rate	[110]
Pei	2018	Graphite foil	H_2SO_4	<5 min	Room temperature	High efficiency	[111]
Ranjan	2018	Graphite	H_2SO_4, H_3PO_4, $KmnO_4$	<24 h	<RT-35–95	Cooled exothermal reaction to make the process safe	[112]

The most preferred methods are Brodie [96], Staudenmaier [97], and Hummers [98], as shown in Figure 11. From these familiar methods, a number of variations have been derived to improve the overall yield and quality of the GO. In 1859, Brodie used graphite as the starting material for the synthesis of graphene oxide (GO). In his experimental work, he used $KclO_4$ (strong oxidizing agent) along with nitric acid and heated the content at 60 °C for 3–4 days [96]. The GO obtained was soluble in pure or basic water. The chemical

composition showed mainly carbon, oxygen, and hydrogen with the general formula $C_{11}H_4O_5$. After nearly four decades, in 1898, Staudenmaier and Hoffmann modified Brodie's method and trimmed down the reaction time of graphene oxide synthesis from 4 days to 2 days [97]. The nitric acid used in Brodie method was also replaced with sulfuric acid, which further reduced the liberation of toxic gases such as NO_2 or N_2O_4.

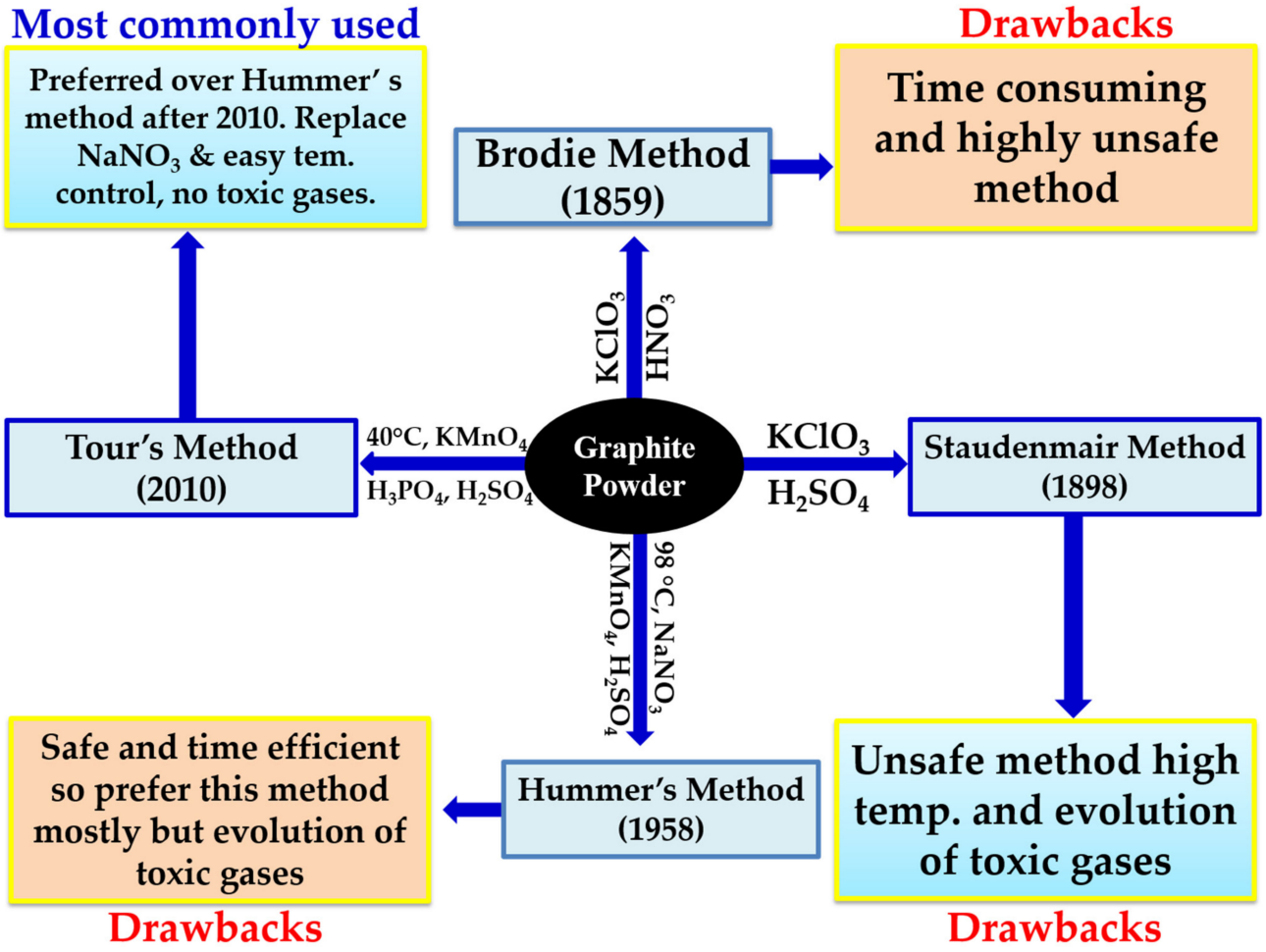

Figure 11. Schematic representation of the synthesis of graphene oxide with different methods.

In 1958, Hummer reduced the reaction time from 2 days to 12 h by using $KmnO_4$ as the oxidizing agent instead of $KclO_4$, followed by the addition of sodium nitrate, but the problem of toxic gases still remains a challenge [98]. Further, in 2010, at Rice University, Tour's group [102] replaced sodium nitrate with phosphoric acid and increased the amount of $KmnO_4$. This improvement made the process eco-friendly, as it completely stops the release of toxic gases such as NO_2, N_2O_4 or ClO_2, along with easy temperature control and better yield [102]. In addition to this, the GO suspension obtained was treated with hydrogen peroxide (H_2O_2) to eliminate all impurities due to permanganate and manganese dioxide.

Furthermore, the final color of the product GO varies from army green to light yellow, depending on the carbon-to-oxygen ratios [113], as depicted in Table 3.

Table 3. Effect of acid concentration, reaction temperature, reaction time, and the quantity of the oxidizing agent on the oxidation of graphene [113].

S. No.	Source of Carbon	H_2SO_4 (in mL)	Other Ingredients	Temp. (in °C)	Time (in h)	C:O	Colour of GO Obtained
1	Graphite	15.0	1.0 g $Na_2Cr_2O_7$	30	72	16:1	Black
2	Graphite	15.0	4.0 g $Na_2Cr_2O_7$	30	72	3.4:1	Black
3	Graphite	15.0	15.0 mL 70% HNO_3 3.0 g $KmnO_4$,	30	24	–	Black
4	Graphite	20.0	11.0 g $KclO_3$, 10.0 mL 70% HNO_3	0–60	33	3.1:1	Midnight green
5	Graphite	30.0	3.0 g $KmnO_4$,1.0 g $NaNO_3$	30	2	3.0:1	Bluish green
6	Graphite	30.0	3.0 g $KmnO_4$,1.0 g $NaNO_3$	45	1	–	Green
7	Graphite	22.5	3.0 g $KmnO_4$,1.0 g $NaNO_3$	45	1	–	Brittle yellow
8	Graphite	22.5	3.0 g $KmnO_4$,0.5 g $NaNO_3$	45	1	–	Yellow
9	Graphite	22.5	3.0 g $KmnO_4$,0.5 g $NaNO_3$	45	0.5	2.3:1	Yellow
10	Graphite	22.5	3.0 g $KmnO_4$,0.5 g $NaNO_3$	35	0.5	2.05:1	Bright yellow
11	Graphite	22.5	3.0 g $KmnO_4$, 1.0 g fuming HNO_3	35	1	–	Bright yellow
12	Graphite	22.5	3.0 g $KmnO_4$, 1.0 g $BaNO_3$	45	2	–	Light green

3.1.1. Post-Synthesis Treatment of GO

The post-synthesis treatment or workup of GO is a must, as the synthesized GO contains a noticeable amount of impurities, viz, the starting material (graphite), oxidizing agents, and the acids [114]. The workup of the graphene oxide could be performed via filtration and centrifugation techniques [114–116]. The common soluble contaminants, viz, ions of metal, sulfate, nitrate, phosphate, and manganese (IV) were removed by washing with a dilute HCL solution a number of times [114–116]. After each wash, GO was recuperated either by vacuum filtration or by centrifugation. Finally, the residues of HCl trapped inside GO were removed by washing with a sufficient quantity of de-ionized water [116–120]. Chen et al. carried out the final washing of GO with a HCl solution (5–10%) through filter paper supported on the funnel [117]. The key features of the process were that it offers high-quality GO totally free from sulfate, phosphate, manganese, and metal ions. Hirata et al. further improved the finishing washing step after centrifugation by giving the final wash with H_2SO_4 and H_2O_2 solutions [121].

3.1.2. Effect of Various Temperatures on the Oxidation Level of GO

Various properties of GO, viz, electrical conductivity, band gap energy, transparency, optical properties, and surface charge are deeply influenced by the content of oxygen in carbonyl moieties present in GO after the oxidation of graphene [122–124]. These oxygen-containing functional groups act as excellent nucleation sites for the growth of inorganic materials over the surface of GO [125–127]. Therefore, to enhance the properties of GO sheets for various applications, it is required to control the oxidation of graphite to tune the amount of oxygen functional groups. This oxygen content on graphene can be controlled by the temperature maintained during the oxidation process of graphene [128–130]. This has been proven by the research carried out by Shin and co-worker in 2012 and Bannov et al. in 2014 [131–133]. Shin and co-worker prepared the GO sheets using the modified Hummers method, performed at different oxidation temperatures, as shown in Table 4. According to their procedure, the addition of cold concentrated sulfuric acid and potassium permanganate in a pre-oxidized graphite powder reaction mixture was stirred at 35 °C for two hours. This temperature was changed to 20 °C and 27 °C, respectively, for other samples [132,134]. From the elemental analysis, it was observed that more functional groups were formed during the oxidation process at higher oxidation temperatures. Further, these functional groups act as first-class nucleation sites for the expansion of inorganic materials like zinc oxide (ZnO), silica (SiO_2), and titania (TiO_2). In conclusion, it can be said that, to further enhance the properties of GO sheets for various applications, it is necessary to control the oxidation of graphite to tune the amount of oxygen functional groups [122–128].

Table 4. Analysis of the elements present in different samples at various temperatures [131].

Elements Present in GO (Weight %)	Sample 1	Sample 2	Sample 3
	Temperature 35 °C	Temperature 27 °C	Temperature 20 °C
Carbon	44.09	45.51	44.55
Oxygen	49.92	48.93	47.16
Hydrogen	3.30	2.96	3.02
Atomic ratio of carbon and oxygen	1.18	1.24	1.26

3.2. Structural Aspects of GO

Various structural models of GO, as shown in Figure 12, have been proposed and were refined over the years by the advancement of characterization techniques and technologies. The structural history of GO started in 1936, when Hofmann and Rudolf [135] proposed the first structure of GO in which epoxy groups were unsystematically spotted over the graphene sheets, and then in 1946, Ruess [136] restructured the Hofmann model by introducing hydroxyl moieties and the alternation of the basal plane structure from an sp^2 to an sp^3 hybridized carbon system.

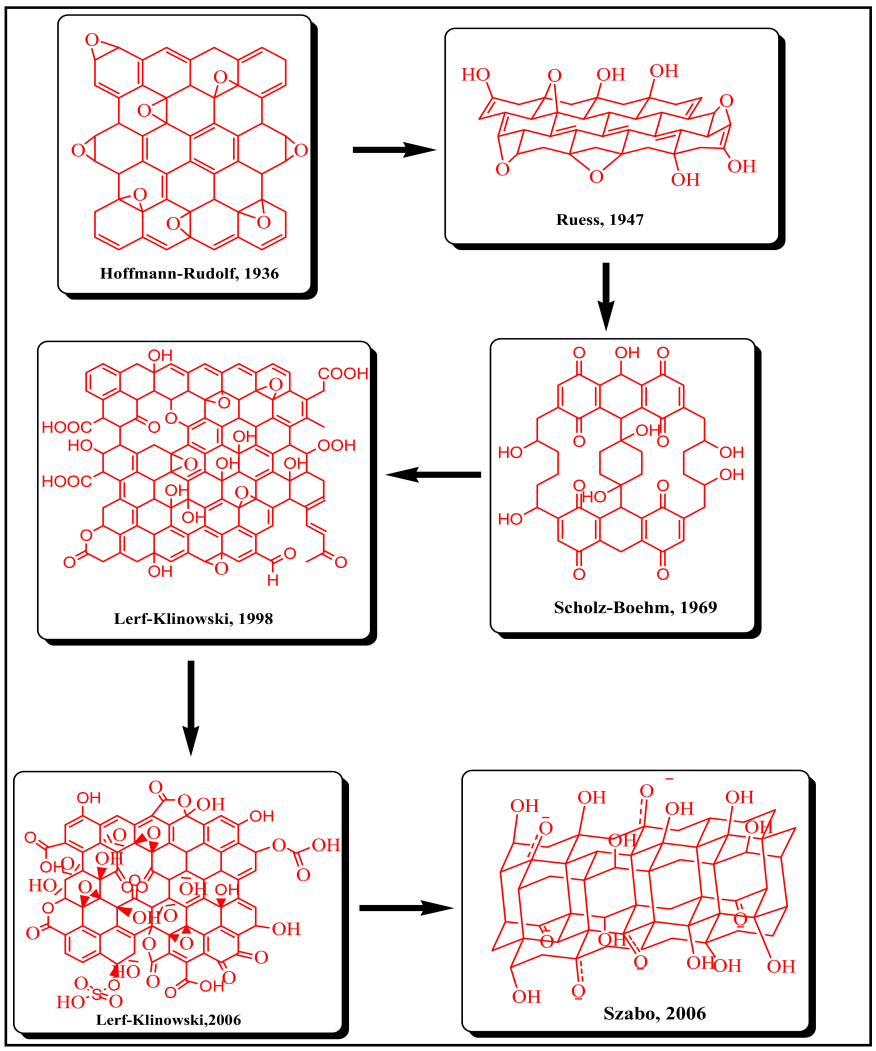

Figure 12. Schematic representation of the year-wise progress in proposed structures of graphene oxide [135–142].

Scholz and Boehm in 1969 [137] proposed a GO structure that was less ordered, having C=C and periodically cleaved C-C bonds within the channeled carbon layers labeled with carbonyl and hydroxyl groups. Further, in 1994, Nakajima and Matsuo [138] presented a graphite intercalation compound (GIC) to look like a lattice framework. Adding to the history, in 1998, Lerf and Klinowski et al. (L–K model) [139,140] proposed a uniform carbon lattice framework GO structure with randomly distributed benzene rings having attached epoxides, carboxyl, and hydroxyl groups. Thereafter, in 2006, Szabó and coworkers [141] put forward a carboxylic-acid-free model comprising two distinct domains: a trans-linked cyclohexyl species interspersed with tertiary alcohols, 1,3-ethers, and a keto/quinoidal species corrugated network. Even closer to the present time, in 2018, Liu et al. [142] experimentally noticed oxygen bonding and evidenced the C=O bonds on the edge and plane of GO, confirming parts of earlier proposed models, especially the L–K model.

Among the above-discussed models from 1936 to 2018, the L–K model has been accepted the most, due to good interpretability over the majority of experimental observations and the ease of further adaption and modification.

3.3. Characterization of GO

In order to authenticate the synthesis of GO and to analyze its chemical configuration, a range of characterization techniques have been employed by numerous research groups. For example, in order to achieve the information of size and surface morphology of graphene oxide, SEM, TEM, and AFM were used abroad [143–147]. With respect to the elemental analysis of graphene oxide, quantitative XPS, EDX, and inductively coupled plasma mass spectrometry (ICP-MS) were utilized generally [148–156]. Additionally, Raman spectra, XRD, and FTIR spectra are widely used to point out the graphene oxide chemical structure [156–160]. To get additional details about the properties of graphene oxide, TGA, and Zeta potential were also engaged by various research groups to evaluate its thermal stability and electrochemical property. More detailed explanations about these above-mentioned techniques are summarized in Table 5 and Figure 13.

Table 5. Various techniques for the characterization of GO.

Technique Used to Characterize Graphene Oxide	Information Obtained	Properties of Compound Observed	References
SEM	Lateral size distribution of GO sheets, showing the structural morphology of GO	Micromorphology and size of graphene oxide	[146]
TEM	Morphology of GO (wrinkles) and single-layered GO sheets.		[147]
AFM	Lateral size and thickness of GO sheets		[148]
TGA	Thermal stability of GO	Thermal stability	[149,150]
XPS	Quantitatively analyze the chemical composition of elements present in GO	Chemical structure of GO	[151–156]
FTIR	Characteristic bands corresponding to carbonyl functional groups, confirmed the successful synthesis of GO		[157,158]
XRD	Crystalline structures of the GO nanosheets and the inter-sheet distance of GO		[159,160]
Raman spectroscopy	Analyzing the chemical structure of GO combined with XPS, FTIR, XRD, ICP-MS.		[161,162]
UV spectroscopy	Help in structure identify	Presence of conjugated and non-bonding electrons	[163]

Abbreviations: SEM: scanning electron microscopy, TEM: transmission electron microscopy, XRD: X-ray crystallography, AFM: atomic force microscopy, TGA: thermogravimetric analysis, XPS: X-ray photoelectron spectroscopy, FTIR: Fourier transform infrared spectroscopy, UV: ultraviolet.

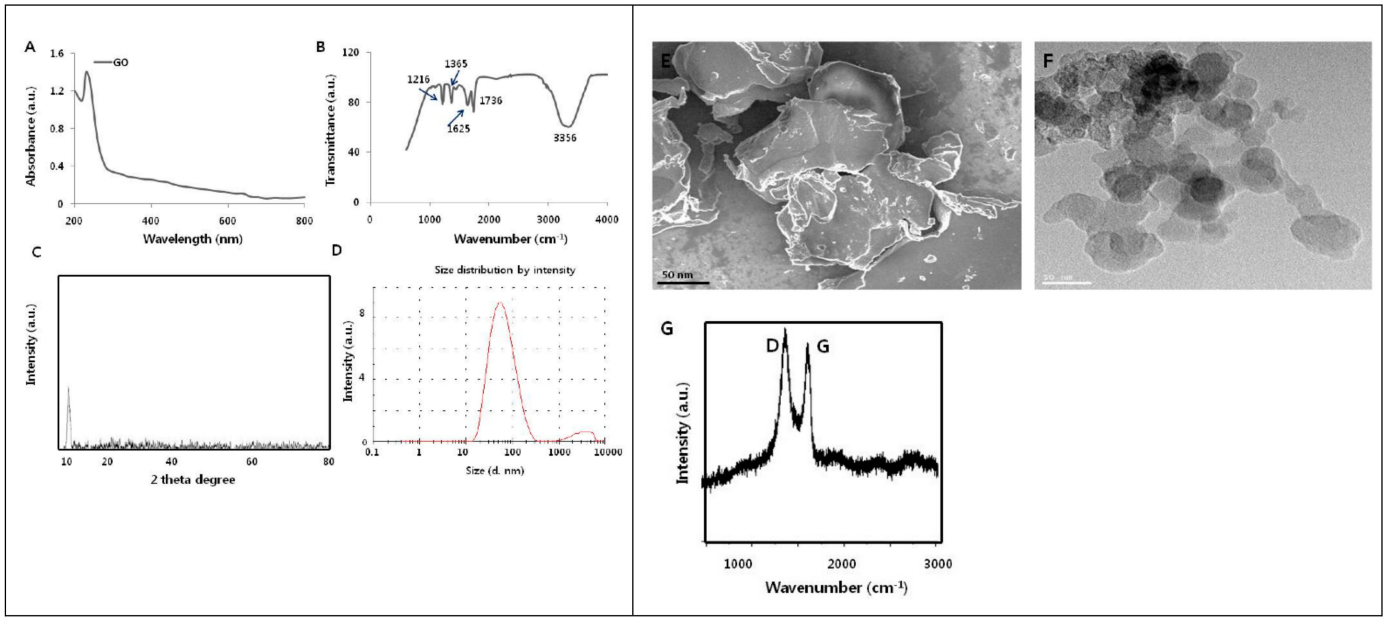

Figure 13. Schematic representation of the various characterizations of graphene oxide. (**A**) UV–visible spectrum, (**B**) FTIR spectrum, (**C**) X-ray diffraction images, (**D**) dynamic light-scattering analysis, (**E**) scanning electron microscopy, (**F**) transmission electron microscopy, (**G**) Raman spectrum [Reprinted with permission from ref. [164], Gurunathan, S.; Arsalan Iqbal, M.; Qasim, M.; Park, C.H.; Yoo, H.; Hwang, J.H.; Uhm, S.J.; Song, H.; Park, C.; Do, J.T.; Choi, Y.; Kim, J.-H.; Hong, K. Evaluation of Graphene Oxide Induced Cellular Toxicity and Transcriptome Analysis in Human Embryonic Kidney Cells. *Nanomaterials* **2019**, *9*, 969. https://doi.org/10.3390/nano9070969] Copyright © MDPI].

4. GO–Metal Oxide Nanocomposite Tailoring for Enhanced Water Purification Applications

Graphene oxide (GO) is no doubt a rising star material for nano-building and has shown great potential in membrane technology for water purification [164–166]. The properties of GO can be extra enhanced by modifications with adding a little sum of divalent alkaline earth metal ions bonded to the functional groups of GO layers [167]. These divalent metal ions act as a cross-linking building block between two adjacent carboxyl moieties of the GO layers and increase their solidity as well as stability. GO can also form composites when blended with carbon nanotubes, metal and their oxides, polymers, and some organic molecules, which work as spacers to prevent GOs restacking and helps in making the graphene material more porous [168–173].

The purification ability of an adsorption process depends on the properties of the adsorbent used. Some functional groups, viz, -C=O, -COOH, -OH, -C-O-C on the graphene oxide surface make GO an excellent adsorbent. Further, due to the huge surface area, a large number of active binding sites and the electron-rich environment of GO nanocomposites have been successfully employed for the adsorption of various pollutants, including pesticides, heavy metals ions, different types of organic dyes, and other organic pollutants [167–169]. Figure 14 highlights the different interactions between active sites and the pollutant molecules [169].

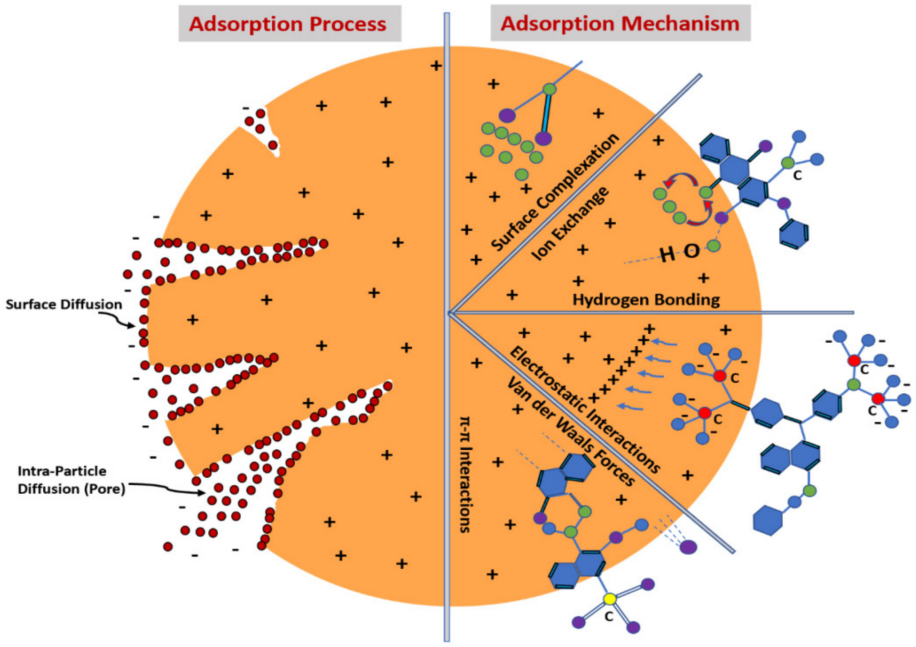

Figure 14. Schematic representation of the adsorption process and its mechanism for the adsorption of pollutants [Reprinted with permission from ref. [169], Hamad, H.N.; Idrus, S. Recent Developments in the Application of Bio-Waste-Derived Adsorbents for the Removal of Methylene Blue from Wastewater: A Review. *Polymers* **2022**, *14*, 783. https://doi.org/10.3390/polym14040783], Copyright © MDPI].

In the present time, the fast development of industries even in the countryside causes the contamination of natural water reservoirs through the ejection of poisonous industrial by-products [164–166]. Therefore, the photocatalytic decomposition of industrial organic by-products is another encouraging technique to eradicate this problem. The word 'photocatalytic decomposition' is referred towards the complete conversion of harmful and less-likely-degradable contaminants into harmless compounds. Heterogeneous photocatalysis involves organic synthesis, water-splitting, photo-reduction, hydrogen transfer, disinfection, water detoxification, gaseous pollutant eradication, etc. The different metal oxide nanoparticles utilized along with GO in the last two to three decades are of silver oxide, titanium dioxide, zinc oxide, copper oxide, aluminum oxide, iron oxide, and zirconium dioxide have also been reported [174,175]. We have reviewed some features of GO as an adsorbent for dyes, metal ions, antibacterial activities, and environmental applications as shown in Table 6. In gas detection activities, graphene-based nanomaterials have been extensively investigated because of their high sensitivity toward various gaseous species. Few-layered hydrophilic sheets of graphene oxide manifest amazing adsorption behavior towards miscellaneous harmful gases such as CO_2, CO, NO_2, and NH_3 [176].

The combination of silver–graphene oxide (Ag/GO) nanocomposites has been reported as an excellent antibacterial agent for water disinfection. According to Sun. et al., the Ag/GO nanocomposite has been further developed for an antibacterial water purification membrane [177]. The graphene oxide sheets were used as an adsorbent for the rapid uptake of four various pesticides from water samples and might be used as a good antioxidant and an antibacterial agent [178]. In addition to this, the SiO_2/GO nanocomposite showed a major improvement in terms of water flux, pollutant rejection, and antifouling tendency in membranes [179]. Moreover, the combination of TiO_2/GO also shows a vast performance in different aspects such as hydrophilicity, water permeability, and fouling resistance [180]. Besides, the synthesis of the ZnO–GO combination has been shown to have enhanced photocatalytic and antimicrobial activity. ZnO nanoparticles can also be used as a water-body restoration material, and it can diminish up to 97% of MB dye under ultraviolet radiation conditions.

Table 6. Some recently published studies on GO–metal oxide nanocomposites and major pollutant trapped for environmental remediation.

GO/Metal Oxide Nanocomposites	Main Pollutant Trapped	Achievements	Reference
GO–silver oxide	Cyclohexane	By using GO–Ag composities as photocatalysts, 37.0% conversion and 94.0% selectivity of cyclohexane to cyclohexanol was achieved.	[181]
Graphene-supported Fe–Mg oxide composite	Arsenic heavy metal ions	The prepared composite exhibited the significant fast adsorption of arsenic with exceptional durability and recyclability.	[182]
GO/Fe_3O_4	Methylene blue and rhodamine B dyes	The dye removal rate for methylene blue was nearly 100%, while for rhodamine B, it was about 90%.	[183]
GO–$MnFe_2O_4$	Pb(II), As(III), and As(V) heavy metal ions	The exceptional adsorption property was due to a combination of the unique layered nature (allowing the maximum surface area) of the hybrid system and the good adsorption capabilities of nanoparticles.	[184]
GO–$ZrO(OH)_2$	As(III) and As(V) heavy metal ions	The GO–$ZrO(OH)_2$ nanocomposite showed a high adsorption capacity in a wide pH range, and the monolayer adsorption amounts were 95.15 and 84.89 mg/g for As(III) and As(V).	[185]
GO–iron oxides	Pb(II) heavy metal ion	The GO–iron oxide nanocomposite acts as a good adsorbent for Pb(II).	[186]
GO–TiO_2	Zn^{2+}, Cd^{2+}, and Pb^{2+} heavy metal ions	The various and dense oxygenated moieties on the GO surface enhanced its capacity to absorb heavy metal ions.	[187]
Graphene–ZnO	Methyl orange dye	The maximum photocatalytic degradation efficiency of methyl orange was 97.1% and 98.6% under UV and sunlight, respectively.	[188]
ZnO–GO/nanocellulose	Ciprofloxacin organic pollutant	The synthesized nanocomposite exhibited enhanced adsorption and photocatalytic performance against ciprofloxacin.	[189]
GO/goethite	Tylosin organic pollutant	The degradation efficiency of the antibiotic by the synthesized composite was 84% after 120 min.	[190]
CuO–CeO_2/GO	Methyl orange dye	The nanocomposite showed better catalytic activity than pure CuO and CuO/GO in the presence of H_2O_2 under visible light irradiation.	[191]

Inclusion of GO–Metal Oxide Nanocomposites into Polymeric Membranes for Enhanced Performance and Application in Different Fields

Over the last few decades, enormous efforts were made to synthesize different types of membranes that could be further employed for a number of applications, viz, drinking-water filtration, use in food [192], the beverage and textile industries [193], petroleum refining [194], paint, and adhesive and solvent recovery stations [195], as shown in Figure 15.

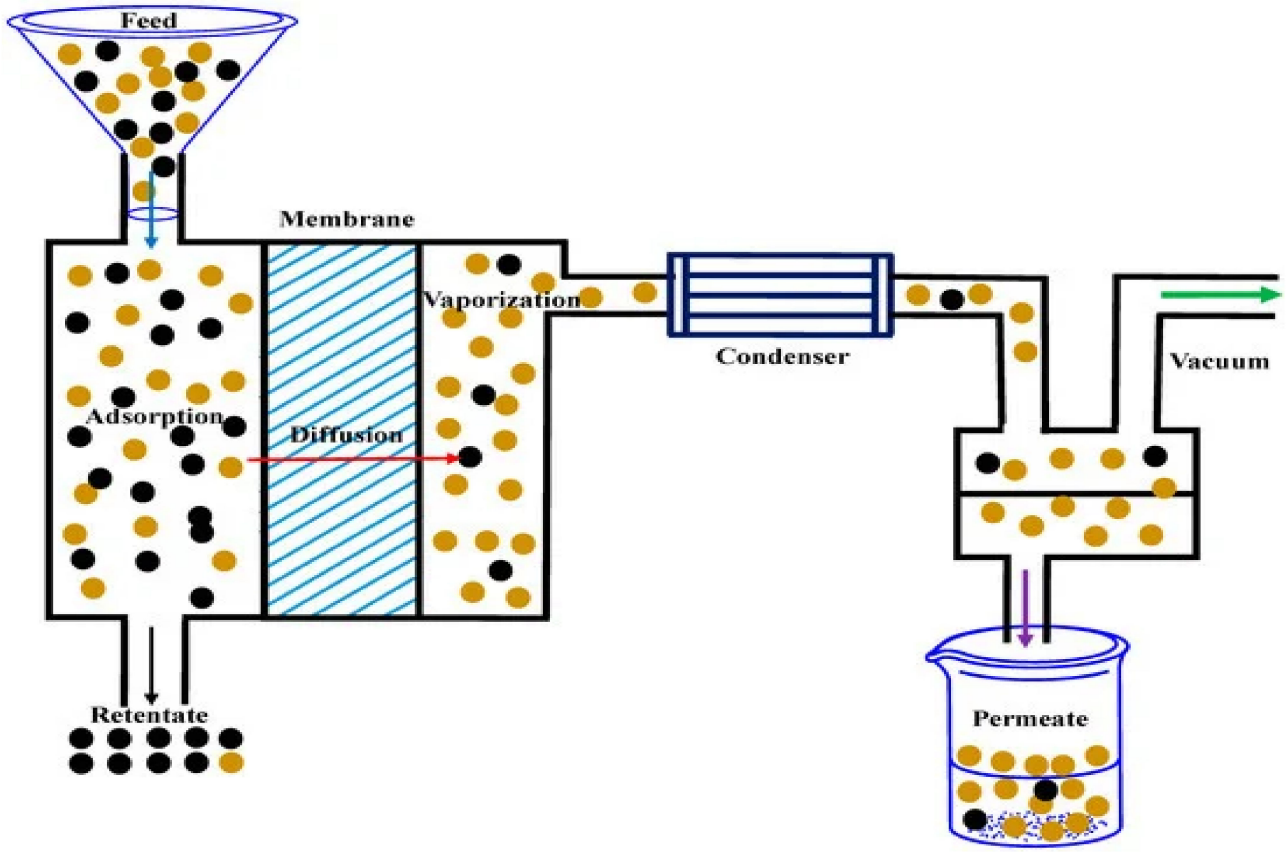

Figure 15. Schematic representation of the basic purification setup with a membrane [Reprinted with permission from ref. [196], Roy, S.; Singha, N.R. Polymeric Nanocomposite Membranes for Next Generation Pervaporation Process: Strategies, Challenges and Future Prospects. *Membranes* **2017**, *7*,53. https://doi.org/10.3390/membranes7030053], Copyright © MDPI].

Despite the good success in the membrane filtration technology, some difficulties and drawbacks [197–201] still need to be studied and discussed. The main drawbacks that limit their application at large scale are membrane fouling [200], membrane choking, and, finally, membrane crumbling. Among these, membrane fouling is the real beginning of the problem [200]. The invasion of bacteria and, further, their colonization on the membrane surface leads to the formation of a microbial biofilm [198], clogging the membrane pores and blocking and restricting the water flow through it [199]. Furthermore, once the microbial biofilm is formed, it becomes quite difficult to remove it. As a result, a large amount of cleaning agents are used, which increase the operation and maintenance costs [198–200]. Numerous research groups have tried different technologies to fabricate the membrane, viz; interfacial polymerization, track-etching, coating, stretching, phase inversion, and electro-spinning for the modification and improvement of the membrane surfaces, but it still requires a lots of improvement [202–205]. Some common techniques used to fabricate the membranes were shown in Figure 16.

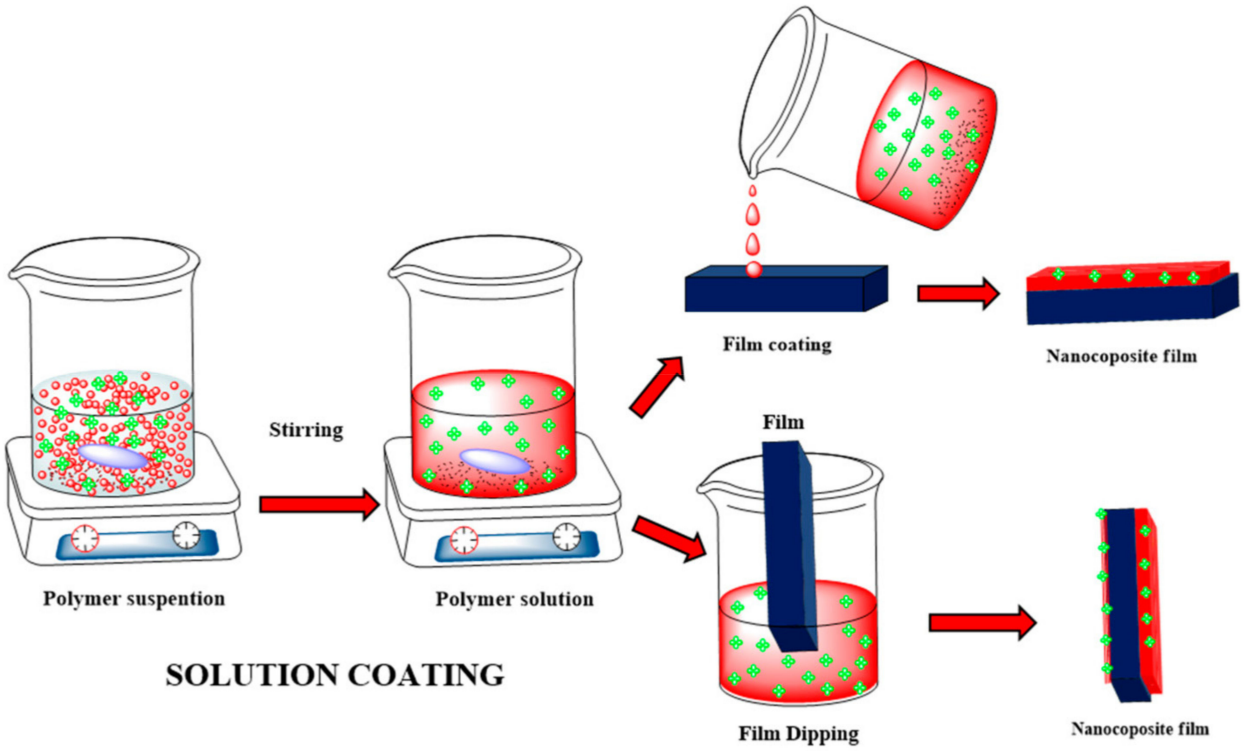

Figure 16. Schematic representation of the fabrication of a polymeric membrane [Reprinted with permission from ref. [196], Roy, S.; Singha, N.R. Polymeric Nanocomposite Membranes for Next Generation Pervaporation Process: Strategies, Challenges and Future Prospects. *Membranes* **2017**, *7*, 53. https://doi.org/10.3390/membranes7030053], Copyright © MDPI].

Further, various types of polymers are tried as a core material, along with organic solvents and inorganic metal oxides, as shown in Table 7, to remove the above-mentioned limitations. Polymers, such as polyvinylidine fluoride, polysulfone, polyethersulfone, polyacrylonitrile, polypropylene, and polytetrafluoroethylene, offer a great design with high flexibility and stability to the membrane [206–210]. Furthermore, to improve the porosity, antibacterial, and anti-fungal activity, other additives such as metal oxide/graphene oxide nanocomposites and organic solvents were incooperated in membrane synthesis by numerous research groups [209–212].

Nanoparticles may be either coated onto the membrane surface or dispersed in the polymer solution before membrane casting, as shown in Figure 16. Dispersing the GO–metal oxide nanocomposites into the polymer generally forms these composite membranes that are a suitable tool to improve the performance, such as permeability and selectivity, of polymeric membranes, due to changes in the surface properties of membranes, influencing the separation performance, excellent rejection of pollutants, and better antifouling behavior, as shown in Figure 17 [208–216].

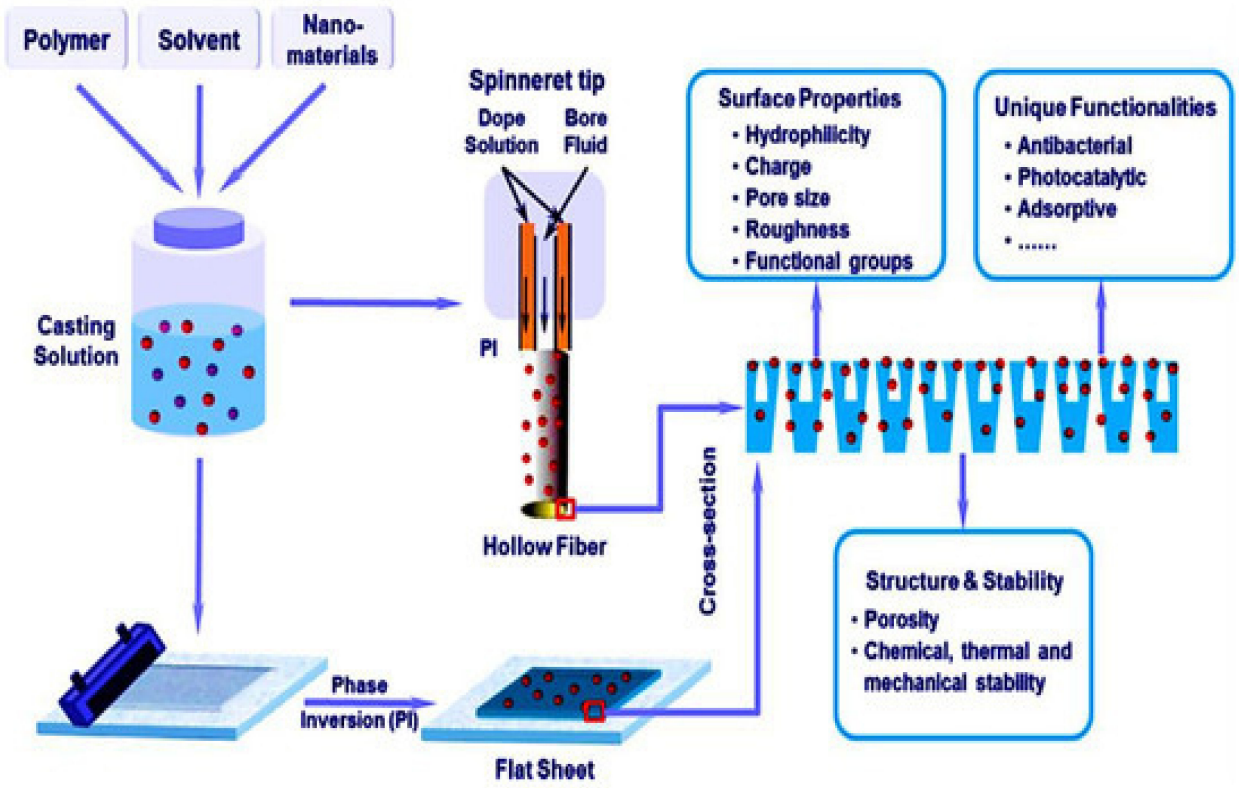

Figure 17. Schematic representation of the fabrication of a polymeric nanocomposite membrane, along with its surface properties [Reprinted with permission from ref. [87], Kausar, A.; Bocchetta, P. Polymer/Graphene Nanocomposite Membranes: Status and Emerging Prospects. *J. Compos. Sci.* **2022**, *6*, 76. https://doi.org/10.3390/jcs6030076, Copyright © MDPI].

Table 7. Different polymeric membranes decorated with metal oxide nanocomposites.

Nanoparticle Used in Membrane	Membrane Type	Application	Polymer Used for Membrane	Reference
ZnO	MF	Treatment of synthetic wastewater	PVDF	[217]
		Removal of copper ions from water		[218]
		Removal of COD from wastewater		[219]
	UF	Removal of HA	PES, PSF	[220,221]
		Removal of salts	PA	[222]
		Evaluation of antifouling properties in composite membranes for water treatment. Mixture model: BSA	PVDF	[223]

Table 7. *Cont.*

Nanoparticle Used in Membrane	Membrane Type	Application	Polymer Used for Membrane	Reference
		Removal of pollutants sodium alginate, BSA, and humic acid (HA)	PES	[224]
		Evaluation of antifouling properties in composite membranes for water treatment. Mixture model: BSA	PES	[225]
		Evaluation of antifouling properties in composite membranes for water treatment. Mixture model: BSA	PVA	[226]
	NF	Removal of HA	PES	[227]
		Water filteration	PVP	[228]
		Removal of inorganic salts and HA	PVDF	[229]
	RO	Removal of salt, bivalent ions (Ca^{2+} SO_4^{2-} and Mg^{2+}), monovalent ions (Cl^- and Na^+), and bacterial retention	PA	[230–232]
	FO	Removal of salts, desalination	PVDF	[230,231]
GO	MF	Treatment of effluents with high-dye content and water filtration	PSF, PVDF	[233,234]
	UF	Treatment of distillery effluent	PES	[235]
		Natural organic matter removal	PA, PVDF	[236]
	NF	Evaluation of dye-removal capacity for water treatment	PES	[237]

Table 7. *Cont.*

Nanoparticle Used in Membrane	Membrane Type	Application	Polymer Used for Membrane	Reference
	RO	Desalination: Salt removal (NaCl, $CaCl_2$, and Na_2SO_4)	PSF	[238,239]
	FO	Possible prospect for the desalination of sea water	PA	[240]
Graphene	UF	Wastewater treatment	PSF	[241]
	NF	Water purification	PVDF	[242]
$AgNO_3$	UF	Reduction of the microbial load of raw milk during the concentration process by the UF process	PES	[243]
		Evaluation of antifouling properties in composite membranes for water treatment. Mixture model: BSA	PSF	[244]
AgNPs	UF	Evaluation of antifouling and antibacterial properties in composite membranes for water treatment. Model bacteria: E. coli	PES, PSF, CA	[244,245]
$AgNO_3$	RO	Evaluation of antibacterial properties and the removal of salt (NaCl). Model bacteria: E. coli and Bacillus subtilis	PA/PSF/PET	[246,247]

Table 7. *Cont.*

Nanoparticle Used in Membrane	Membrane Type	Application	Polymer Used for Membrane	Reference
CuNPs	UF	Treatment of wastewater (sludge filtration) and the evaluation of antifouling properties in composite membranes for water treatment. Mixture model: BSA	PES	[248]
	RO	Evaluation of antibacterial properties in composite membranes for water treatment and the removal of salt (NaCl). Model bacteria: E. coli, P. aeruginosa, and S. aureus.	PA	[248]
TiO_2-NPs	NF	Wastewater treatment application	PES	[249]
	UF	Evaluation of antifouling properties in composite membranes for water treatment. Mixture model: BSA, PEG, and $MgSO_4$	PVDF	[250]
		Evaluation of UV-cleaning properties and antifouling properties. Mixture model: red dye and BSA	PA	[251]

Abbreviations: BSA—bovine serum albumin, CA—cellulose acetate, HA—hummic acid, PA—polyamide, PAA—poly(acrylic acid), PAI—poly(amide-imide), PAN—polyacrylonitrile, PEI—polyethyleneimine, PE—polyethylene, PEG—polyethylene glycol, PSF—polysulfone, PES—polyethersulfone, PVA—polyvinyl alcohol, PVDF—polyvinylidine fluoride, PVP—polyvinylpyrrolidone, PVC—polyvinyl chloride, PP—polypropylene, NF—nanofiltration, RO—reverse osmosis, UF—ultrafiltration, ZnO—zinc oxide, GO—graphene oxide, MF—microfiltration.

5. Challenges and Futuristic Aspects

The graphene-oxide-based nanomaterial, along with metal oxide nanocomposites, deposited on polymeric membranes have achieved excellent appreciation as a water purifier, but there are still few drawbacks and challenges that confine their use at a large scale.

Various routes of GO synthesis have been discussed in the research, and each route has given GO that is good quality-wise, but the overall yield is low. An improvement in the overall yield is a major concern. It needs to be addressed sooner, if we want to use GO in large-scale applications.

The second challenge is the aggregation of the GO–metal oxide nanomaterials on the membrane surfaces, which diminishes the active surface area, the porosity, and the overall performance of the membrane. Over the last two decade or so, many research [197–202] groups have made attempts to remove this challenge by making alterations in the synthesis of graphene oxide–metal oxide nanomaterial and decorated it on the polymeric membranes with different methods [201–205].

The third and the most important challenge is related to membrane strength, membrane-wetting, and membrane-fouling due to colloids and particles present in the feed flow, which tends to significantly reduce membrane performance, increase operating costs, and shorten membrane life.

6. Conclusions

In recent years, many research groups are paying attention towards graphene because of its sole physicochemical properties, viz, high tensile strength, better electrical and thermal conductivity, fast carrier mobility, elasticity, and about 97% optical transparency. In this review article, a brief account on the structure, properties, synthesis, characterizations, and applications of graphene, graphene oxide, and GO–metal oxide-decorated polymeric membranes are discussed. Since its discovery in 2004, graphene has resulted in a wide range of applications in various fields such as solar cells, supercapacitors, sensors, batteries, and water-purification technologies. In addition, the presence of an abundance of oxygenated moieties on the GO nanoparticles imparts a high negative charge density over the GO surface and improves the adsorption quality. The addition of the graphene-based materials in the polymeric membrane-based water-purification processes enhanced the positive impact on the hydrophilicity and the antifouling and antibacterial properties of the membranes. Furthermore, GO–metal oxide nanocomposites with increased antibacterial effects and low toxicity can be employed efficiently as disinfection agents in the surface coatings on numerous membranes to effectively suppress bacterial growth.

The aim of this review was to study the development of a novel high-tech membrane using a polymer decorated with a GO–metal nanocomposite to improve the overall membrane performance, including antibacterial properties, antifouling, porosity, and the surface hydrophilicity of the membrane.

Funding: Ahmad Umar and A. A. Ibrahim would like to thank the Deanship of Scientific Research at Najran University, Najran, Kingdom of Saudi Arabia for funds under the Research Collaboration funding program grant no. NU/RG/SERC/11/1.

Acknowledgments: The authors are thankful to Head of Chemistry Department, Maharishi Markandeshwar (Deemed to be University), Mullana Ambala, India, for providing research facilities.

Conflicts of Interest: The authors declare no conflict of interest.

References

1. Xu, S.; Che, J.; An, Y.; Zhu, T.; Pang, L.; Liu, X.; Li, X.; Lv, M. Research and Preparation of Graphene Foam Based on Passive Ultra-Low Energy Consumption Building New Ultra-Thin External Wall Insulation Material. *J. Nanoelectron. Optoelectron.* **2021**, *16*, 1467–1474. [CrossRef]
2. Banciu, C.A.; Nastase, F.; Istrate, A.-I.; Veca, L.M. 3D Graphene Foam by Chemical Vapor Deposition: Synthesis, Properties, and Energy-Related Applications. *Molecules* **2022**, *27*, 3634. [CrossRef] [PubMed]
3. Umar, A.; Kumar, S.A.; Inbanathan, S.S.R.; Modarres, M.; Kumar, R.; Algadi, H.; Baskoutas, S. Enhanced sunlight-driven photocatalytic, supercapacitor and antibacterial applications based on graphene oxide and magnetite-graphene oxide nanocomposites. *Ceram. Int.* **2022**, *48*, 29349–29358. [CrossRef]
4. Isaeva, V.I.; Vedenyapina, M.D.; Kurmysheva, A.Y.; Weichgrebe, D.; Nair, R.R.; Nguyen, N.P.T.; Kustov, L.M. Modern Carbon–Based Materials for Adsorptive Removal of Organic and Inorganic Pollutants from Water and Wastewater. *Molecules* **2021**, *26*, 6628. [CrossRef] [PubMed]
5. Pelosato, R.; Bolognino, I.; Fontana, F.; Sora, I.N. Applications of Heterogeneous Photocatalysis to the Degradation of Oxytetracycline in Water: A Review. *Molecules* **2022**, *27*, 2743. [CrossRef]
6. Huang, H.-H.; Joshi, R.K.; de Silva, K.K.H.; Badam, R.; Yoshimura, M.J. Fabrication of reduced graphene oxide membranes for water desalination. *Membr. Sci.* **2019**, *572*, 12. [CrossRef]

7. Franco, P.; Cardea, S.; Tabernero, A.; De Marco, I. Porous Aerogels and Adsorption of Pollutants from Water and Air: A Review. *Molecules* **2021**, *26*, 4440. [CrossRef]
8. Santoso, E.; Ediati, R.; Kusumawati, Y.; Bahruji, H.; Sulistiono, D.O.; Prasetyoko, D. Mater. *Today Chem.* **2020**, *16*, 100233.
9. Xiao, C.; Li, C.; Hu, J.; Zhu, L. The Application of Carbon Nanomaterials in Sensing, Imaging, Drug Delivery and Therapy for Gynecologic Cancers: An Overview. *Molecules* **2022**, *27*, 4465. [CrossRef]
10. Guo, W.; Umar, A.; Alsaiari, M.A.; Wang, L.; Pei, M. Ultrasensitive and selective label-free aptasensor for the detection of penicillin based on nanoporousPtTi/graphene oxide-Fe_3O_4/MWCNT-Fe_3O_4 nanocomposite. *Microchem. J.* **2020**, *158*, 105270. [CrossRef]
11. Pandey, R.R.; Chusuei, C.C. Carbon Nanotubes, Graphene, and Carbon Dots as Electrochemical Biosensing Composites. *Molecules* **2021**, *26*, 6674. [CrossRef] [PubMed]
12. Hu, H.; Liang, H.; Fan, J.; Guo, L.; Li, H.; de Rooij, N.F.; Umar, A.; Algarni, H.; Wang, Y.; Zhou, G. Assembling Hollow Cactus-Like ZnO Nanorods with Dipole-Modified Graphene Nanosheets for Practical Room-Temperature Formaldehyde Sensing. *ACS Appl. Mater. Interfaces* **2022**, *14*, 13186–13195. [CrossRef] [PubMed]
13. Al Fatease, A.; Guo, W.; Umar, A.; Zhao, C.; Alhamhoom, Y.; Muhsinah, A.B.; Mahnashi, M.H.; Ansari, Z.A. A dual-mode electrochemical aptasensor for the detection of Mucin-1 based on AuNPs-magnetic graphene composite. *Microchem. J.* **2022**, *180*, 107559. [CrossRef]
14. Treerattrakoon, K.; Jiemsakul, T.; Tansarawiput, C.; Pinpradup, P.; Iempridee, T.; Luksirikul, P.; Khoothiam, K.; Dharakul, T.; Japrung, D. Rolling circle amplification and graphene-based sensor-on-a-chip for sensitive detection of serum circulating miRNAs. *Anal. Biochem.* **2019**, *577*, 89. [CrossRef] [PubMed]
15. Cosma, D.; Urda, A.; Radu, T.; Rosu, M.C.; Mihet, M.; Socaci, C. Evaluation of the Photocatalytic Properties of Copper Oxides/Graphene/TiO_2 Nanoparticles Composites. *Molecules* **2022**, *27*, 5803. [CrossRef]
16. Wang, H.-L.; Wang, Z.-G.; Liu, S.-L. Lipid Nanoparticles for mRNA Delivery to Enhance Cancer Immunotherapy. *Molecules* **2022**, *27*, 5607. [CrossRef]
17. Gong, Y.; Li, H.; Pei, W.; Fan, J.; Umar, A.; Al-Assiri, M.S.; Wang, Y.; de Rooij, N.; Zhou, G. Assembly with copper(II) ions and D–π–A molecules on a graphene surface for ultra-fast acetic acid sensing at room temperature. *RSC Adv.* **2019**, *9*, 30432–30438. [CrossRef]
18. Gong, P.; Zhang, L.; Yuan, X.; Liu, X.; Diao, X.; Zhao, Q.; Tian, Z.; Sun, J.; Liu, Z.; You, J. Multifunctional fluorescent PEGylated fluorinated graphene for targeted drug delivery: An experiment and DFT study. *Dye. Pigment.* **2019**, *162*, 573. [CrossRef]
19. Xu, L.; Gai, L.; Yang, F.; Wu, S. Preparation of Nanographene and Its Effect on the Correlation Between N-Terminal Pro Brain-Type Natriuretic Peptide, Peripheral Blood Copeptin Level and Cardiac Function Grading of Patients with Heart Failure. *Sci. Adv. Mater.* **2021**, *13*, 1937–1944. [CrossRef]
20. Patil, T.V.; Patel, D.K.; Dutta, S.D.; Ganguly, K.; Lim, K.-T. Graphene Oxide-Based Stimuli-Responsive Platforms for Biomedical Applications. *Molecules* **2021**, *26*, 2797. [CrossRef]
21. Cirillo, G.; Pantuso, E.; Curcio, M.; Vittorio, O.; Leggio, A.; Iemma, F.; De Filpo, G.; Nicoletta, F.P. Alginate Bioconjugate and Graphene Oxide in Multifunctional Hydrogels for Versatile Biomedical Applications. *Molecules* **2021**, *26*, 1355. [CrossRef]
22. Bahrami, S.; Solouk, A.; Mirzadeh, H.; Seifalian, A.M. Electroconductive polyurethane/graphene nanocomposite for biomedical applications. *Compos. Part B Eng.* **2019**, *168*, 421–431. [CrossRef]
23. Wang, W.; Junior, J.R.P.; Nalesso, P.R.L.; Musson, D.; Cornish, J.; Mendonça, F.; Caetano, G.F.; Bártolo, P. Engineered 3D printed poly (ε-caprolactone)/graphene scaffolds for bone tissue engineering. *Mater. Sci. Eng. C* **2019**, *100*, 759. [CrossRef] [PubMed]
24. Zhang, S.; Zhuang, Y.; Jin, S.; Wang, K. Preparation of Nanoscale Graphene Oxide and Its Application on β-Catenin Expression in Pediatric Osteosarcoma Cells Combine with Probiotics. *Sci. Adv. Mater.* **2021**, *13*, 2131–2137. [CrossRef]
25. Bai, H.; Guo, H.; Wang, J.; Dong, Y.; Liu, B.; Xie, Z.; Guo, F.; Chen, D.; Zhang, R.; Zheng, Y. A room-temperature NO_2 gas sensor based on CuO nanoflakes modified with rGO nanosheets. *Sens. Actuators B Chem.* **2021**, *337*, 129783. [CrossRef]
26. Hussein-Al-Ali, S.H.; Hussein Alali, S.H.; Al-Ani, R.; Alkrad, J.A.; Abudoleh, S.M.; Abdallah Abualassal, Q.I.; Ayoub, R.; Hussein, M.Z.; Bullo, S.; Palanisamy, A. Betulinic Acid-Graphene Oxide Nanocomposites for Cancer Treatment. *Sci. Adv. Mater.* **2021**, *13*, 2138–2148. [CrossRef]
27. Singh, J.; Goyat, R. Graphene oxide: Synthesis, characterization and its applications. *Res. J. Chem. Environ.* **2022**, *26*, 150–156.
28. Wan, X.; Huang, Y.; Chen, Y. Focusing on energy and optoelectronic applications: A journey for graphene and graphene oxide at large scale. *Acc. Chem. Res.* **2012**, *45*, 598–607. [CrossRef]
29. Ramu, A.G.; Umar, A.; Ibrahim, A.A.; Algadi, H.; Ibrahim, Y.S.A.; Choi, Y.W.D. Synthesis of porous 2D layered nickel oxide-reduced graphene oxide (NiO-rGO) hybrid composite for the efficient electrochemical detection of epinephrine in biological fluid. *Environ. Res.* **2021**, *200*, 111366. [CrossRef]
30. Santosh, K.; Sahoo, S.; Wang, N.; Huczko, A. Graphene research and their outputs: Status and prospect. *J. Sci. Adv. Mater. Devices* **2020**, *5*, 10–29, ISSN 2468-2179.
31. Aliofkhazraei, M.; Ali, N.; Milne, W.I.; Ozkan, C.S.; Mitura, S.; Gervasoni, J.L. *Graphene Science Handbook: Fabrication Methods*; CRC Press: Boca Raton, FL, USA, 2016; p. 587.
32. Dasari, B.L.; Nouri, J.M.; Brabazon, D.; Naher, S. Graphene and derivatives–Synthesis techniques, properties and their energy applications. *Energy* **2017**, *140*, 766. [CrossRef]
33. Toh, S.Y.; Loh, K.S.; Kamarudin, S.K.; Daud, W.R.W. Graphene production via electrochemical reduction of graphene oxide: Synthesis and characterization. *Chem. Eng. J.* **2014**, *251*, 422. [CrossRef]

34. Novoselov, K.S.; Geim, A.K.; Morozov, S.V.; Jiang, D.; Zhang, Y.; Dubonos, S.V.; Grigorieva, I.V.; Firsov, A.A. Electric field effect in atomically thin carbon films. *Science* **2004**, *306*, 666. [CrossRef] [PubMed]
35. Ma, J.; Syed, J.A.; Su, D. Hybrid Supercapacitors Based on Self-Assembled Electrochemical Deposition of Reduced Graphene Oxide/Polypyrrole Composite Electrodes. *J. Nanoelectron. Optoelectron.* **2021**, *16*, 949–956. [CrossRef]
36. Taghioskoui, M. Trends in graphene research. *Mater. Today* **2009**, *12*, 34–37. [CrossRef]
37. Bhuyan, M.S.A.; Uddin, M.N.; Islam, M.M.; Bipasha, F.A.; Hossain, S.S. Synthesis of graphene. *Int. Nano Lett.* **2016**, *6*, 65. [CrossRef]
38. Novoselov, K.S.; Fal'ko, V.I.; Colombo, L.; Gellert, P.R.; Schwab, M.G.; Kim, K. A roadmap for graphene. *Nature* **2012**, *490*, 192. [CrossRef]
39. Ibrahim, A.; Klopocinska, A.; Horvat, K.; Abdel Hamid, Z. Graphene-Based Nanocomposites: Synthesis, Mechanical Properties, and Characterizations. *Polymers* **2021**, *13*, 2869. [CrossRef]
40. Yu, P.; Lowe, S.E.; Simon, G.P.; Zhong, Y.L. Electrochemical exfoliation of graphite and production of functional graphene. *Curr. Opin. Colloid Interface Sci.* **2015**, *20*, 329. [CrossRef]
41. Öztürk, A.; Alanyalıoğlu, M. Electrochemical fabrication and amperometric sensor application of graphene sheets. *Superlattices Microstruct.* **2016**, *95*, 56. [CrossRef]
42. Parvez, K.; Li, R.; Puniredd, S.R.; Hernandez, Y.; Hinkel, F.; Wang, S.; Feng, X.; Müllen, K. Electrochemically exfoliated graphene as solution-processable, highly conductive electrodes for organic electronics. *ACS Nano* **2013**, *7*, 3598. [CrossRef] [PubMed]
43. Liu, J.; Yang, H.; Zhen, S.G.; Poh, C.K.; Chaurasia, A.; Luo, J.; Wu, X.; Yeow, E.K.L.; Sahoo, N.G.; Lin, J.; et al. A green approach to the synthesis of high-quality graphene oxide flakes via electrochemical exfoliation of pencil core. *Rsc Adv.* **2013**, *3*, 11745–11750. [CrossRef]
44. Madurani, K.A.; Suprapto, S.; Machrita, N.I.; Bahar, S.L.; Illiya, W.; Kurniawan, F. Progress in Graphene Synthesis and its Application: History, Challenge and the Future Outlook for Research and Industry. *ECS J. Solid State Sci. Technol.* **2020**, *9*, 093013. [CrossRef]
45. Lotya, M.; Hernandez, Y.; King, P.J.; Smith, R.J.; Nicolosi, V.; Karlsson, L.S.; Blighe, F.M.; De, S.; Wang, Z.; McGowern, I.T.; et al. Liquid phase production of graphene by exfoliation of graphite in surfactant/water solutions. *J. Am. Chem. Soc.* **2009**, *131*, 3611–3620. [CrossRef] [PubMed]
46. Ma, J. A Method for Solving the Minimum Vertex Covering Problem Based on Graphene. *J. Nanoelectron. Optoelectron.* **2021**, *16*, 460–465. [CrossRef]
47. Green, A.A.; Hersam, M.C. Solution phase production of graphene with controlled thickness via density differentiation. *Nano Lett.* **2009**, *9*, 4031–4036. [CrossRef]
48. Gürünlü, B.; Taşdelen-Yücedağ, Ç.; Bayramoğlu, M. Graphene Synthesis by Ultrasound Energy-Assisted Exfoliation of Graphite in Various Solvents. *Crystals* **2020**, *10*, 1037. [CrossRef]
49. Lee, C.-W.; Jeong, S.-Y.; Kwon, Y.-W.; Lee, J.-U.; Cho, S.-C.; Shin, B.-S. Fabrication of laser-induced graphene-based multifunctional sensing platform for sweat ion and human motion monitoring. *Sens. Actuators A Phys.* **2022**, *334*, 113320. [CrossRef]
50. Zhang, Z.; Tang, C.; Zhang, K.; Li, H.; Cao, J.; Shao, Z.; Gong, J. Synthesis of $Mn(OH)_2$ Nanosheets on Carbon Cloth for High-Performance Aqueous Zinc-Ion Battery. *J. Nanoelectron. Optoelectron.* **2021**, *16*, 1698–1704. [CrossRef]
51. Hemani, G.K.; Vandenberghe, W.G.; Brennan, B.; Chabal, Y.J.; Walker, A.V.; Wallace, R.M.; Quevedo-Lopez, M.; Fischetti, M.V. Interfacial graphene growth in the Ni/SiO_2 system using pulsed laser deposition. *Appl. Phys. Lett.* **2013**, *103*, 134102. [CrossRef]
52. Cappelli, E.; Orlando, S.; Servidori, M.; Scilletta, C. Nano-graphene structures deposited by N-IR pulsed laser ablation of graphite on Si. *Appl. Surf. Sci.* **2007**, *254*, 1273. [CrossRef]
53. Koh, A.T.; Foong, Y.M.; Chua, D.H. Comparison of the mechanism of low defect few-layer graphene fabricated on different metals by pulsed laser deposition. *Diam. Relat. Mater.* **2012**, *25*, 98–102. [CrossRef]
54. Barcikowski, S.; Devesa, F.; Moldenhauer, K. Impact and structure of literature on nanoparticle generation by laser ablation in liquids. *J. Nanoparticle Res.* **2009**, *11*, 1883–1893. [CrossRef]
55. Barcikowski, S.; Compagnini, G. Advanced nanoparticle generation and excitation by lasers in liquids. *Phys. Chem. Chem. Phys.* **2013**, *15*, 3022. [CrossRef] [PubMed]
56. Nancy, P.; Jose, J.; Joy, N.; Valluvadasan, S.; Philip, R.; Antoine, R.; Thomas, S.; Kalarikkal, N. Fabrication of Silver-Decorated Graphene Oxide Nano-hybrids via Pulsed Laser Ablation with Excellent Antimicrobial and Optical Limiting Performance. *Nanomaterials* **2021**, *11*, 880. [CrossRef]
57. Lim, J.Y.; Mubarak, N.M.; Abdullah, E.C.; Nizamuddin, S.; Khalid, M.; Inamuddin, I.J. Recent trends in the synthesis of graphene and graphene oxide based nanomaterials for removal of heavy metals—A review. *Ind. Eng. Chem.* **2018**, *66*, 29. [CrossRef]
58. Li, X.; Cai, W.; An, J.; Kim, S.; Nah, J.; Yang, D.; Piner, R.; Velamakanni, A.; Jung, I.; Tutuc, E.; et al. Large-area synthesis of high-quality and uniform graphene films on copper foils. *Science* **2009**, *324*, 1312–1314. [CrossRef]
59. Lavin-Lopez, M.P.; Valverde, J.L.; Ordoñez-Lozoya, S.; Paton-Carrero, A.; Romero, A. Role of inert gas in the Cvd-graphene synthesis over polycrystalline nickel foils. *Mater. Chem. Phys.* **2019**, *222*, 173. [CrossRef]
60. Liu, W.; Li, H.; Xu, C.; Khatami, Y.; Banerjee, K. Synthesis of high-quality monolayer and bilayer graphene on copper using chemical vapor deposition. *Carbon* **2011**, *49*, 4122. [CrossRef]
61. Reina, A.; Jia, X.; Ho, J.; Nezich, D.; Son, H.; Bulovic, V.; Dresselhaus, M.S.; Kong, J. Large area, few-layer graphene films on arbitrary substrates by chemical vapor deposition. *Nano Lett.* **2008**, *9*, 30–35. [CrossRef]

62. Chae, S.J.; GüneŞ, F.; Kim, K.K.; Kim, E.S.; Han, G.H.; Kim, S.M.; Shin, H.J.; Yoon, S.M.; Choi, J.Y.; Park, M.H.; et al. Synthesis of large-area graphene layers on poly-nickel substrate by chemical vapor deposition: Wrinkle formation. *Adv. Mater. Weinh.* **2009**, *21*, 2328–2333. [CrossRef]
63. Kim, M.; Safron, N.S.; Han, E.; Arnold, M.S.; Gopalan, P. Fabrication and characterization of large-area, semiconducting nanoperforated graphene materials. *Nano Lett.* **2010**, *10*, 1125–1131. [CrossRef] [PubMed]
64. Guermoune, A.; Chari, T.; Popescu, F.; Sabri, S.S.; Guillemette, J.; Skulason, H.S.; Szkopek, T.; Siaj, M. Chemical vapor deposition synthesis of graphene on copper with methanol, ethanol, and propanol precursors. *Carbon* **2011**, *49*, 4204–4210. [CrossRef]
65. Suk, J.W.; Kitt, A.; Magnuson, C.W.; Hao, Y.; Ahmed, S.; An, J.; Swan, A.K.; Goldberg, B.B.; Ruoff, R.S. Transfer of CVD-grown monolayer graphene onto arbitrary substrates. *ACS Nano* **2011**, *5*, 6916–6924. [CrossRef]
66. Chaitoglou, S.; Bertran, E. Effect of temperature on graphene grown by chemical vapor deposition. *J. Mater. Sci.* **2017**, *52*, 8348–8356. [CrossRef]
67. Saeed, M.; Alshammari, Y.; Majeed, S.A.; Al-Nasrallah, E. Chemical Vapour Deposition of Graphene—Synthesis, Characterisation, and Applications: A Review. *Molecules* **2020**, *25*, 3856. [CrossRef]
68. Wu, X.; Liu, Y.; Yang, H.; Shi, Z. Large-scale synthesis of high-quality graphene sheets by an improved alternating current arc-discharge method. *RSC Adv.* **2016**, *6*, 93119–93124. [CrossRef]
69. Kim, S.; Song, Y.; Wright, J.; Heller, M.J. Graphene bi-and trilayers produced by a novel aqueous arc discharge process. *Carbon* **2016**, *102*, 339. [CrossRef]
70. Cheng, G.-W.; Chu, K.; Chen, J.S.; Tsai, J.T.H. Fabrication of graphene from graphite by a thermal assisted vacuum arc discharge system. *Superlattices Microstruct.* **2017**, *104*, 258. [CrossRef]
71. Tan, H.; Wang, D.; Guo, Y. A Strategy to Synthesize Multilayer Graphene in Arc-Discharge Plasma in a Semi-Opened Environment. *Materials* **2019**, *12*, 2279. [CrossRef]
72. Subrahmanyam, K.S.; Panchakarla, L.S.; Govindaraj, A.; Rao, C.N.R. Simple method of preparing graphene flakes by an arc-discharge method. *J. Phys. Chem. C* **2009**, *113*, 4257. [CrossRef]
73. Kim, S.; Song, Y.; Takahashi, T.; Oh, T.; Heller, M.J. An aqueous single reactor arc discharge process for the synthesis of graphene nanospheres. *Small* **2015**, *11*, 5041. [CrossRef] [PubMed]
74. Zhu, M.; Wang, J.; Holloway, B.C.; Outlaw, R.A.; Zhao, X.; Hou, K.; Shutthanandan, V.; Manos, D.M. A mechanism for carbon nanosheet formation. *Carbon N. Y.* **2007**, *45*, 2229–2234. [CrossRef]
75. Yuan, G.D.; Zhang, W.J.; Yang, Y.; Tang, Y.B.; Li, Y.Q.; Wang, J.X.; Meng, X.M.; He, Z.B.; Wu, C.M.L.; Bello, I.; et al. Graphene sheets via microwave chemical vapor deposition. *Chem. Phys. Lett.* **2009**, *467*, 361–364. [CrossRef]
76. Kim, J.; Ishihara, M.; Koga, Y.; Tsugawa, K.; Hasegawa, M.; Iijima, S. Low-temperature synthesis of large-area graphene-based transparent conductive films using surface wave plasma chemical vapor deposition. *Appl. Phys. Lett.* **2011**, *98*, 091502. [CrossRef]
77. Malesevic, A.; Vitchev, R.; Schouteden, K.; Volodin, A.; Zhang, L.; Tendeloo, G.V.; Vanhulsel, A.; Haesendonck, C.V. Synthesis of few-layer graphene via microwave plas-ma-enhanced chemical vapour deposition. *Nanotechnology* **2008**, *19*, 305604. [CrossRef]
78. Wang, J.; Zhu, M.; Outlaw, R.A.; Zhao, X.; Manos, D.M.; Holloway, B.C. Synthesis of carbon nanosheets by inductively coupled radio-frequency plasma enhanced chemical vapor deposition. *Carbon N. Y.* **2004**, *42*, 2867–2872. [CrossRef]
79. Krivchenko, V.A.; Dvorkin, V.V.; Dzbanovsky, N.N.; Timofeyev, M.A.; Stepanov, A.S.; Rakhimov, A.T.; Suetin, N.V.; Vilkov, O.Y.; Yashina, L.V. Evolution of carbon film structure during its catalyst-free growth in the plasma of direct current glow discharge. *Carbon N. Y.* **2012**, *50*, 1477–1487. [CrossRef]
80. Stefanos Chaitoglou, Roger Amade, Enric Bertran, Insights into the inherent properties of vertical graphene flakes towards hydrogen evolution reaction. *Appl. Surf. Sci.* **2022**, *592*, 153327, ISSN 0169-4332. [CrossRef]
81. Bo, Z.; Yang, Y.; Chen, J.; Yu, K.; Yan, J.; Cen, K. Plasma-enhanced chemical vapor deposition synthesis of vertically oriented graphene nanosheets. *Nanoscale* **2013**, *5*, 5180–5204. [CrossRef]
82. Singh, V.; Joung, D.; Zhai, L.; Das, S.; Khondaker, S.I.; Seal, S. Graphene based materials: Past, present and future. *Prog. Mater. Sci.* **2011**, *56*, 1178–1271. [CrossRef]
83. Yannopoulos, S.N.; Siokou, A.; Nasikas, N.K.; Dracopoulos, V.; Ravani, F.; Papatheodorou, G.N. CO_2-Laser-induced growth of epitaxial graphene on 6H-SiC(0001). *Adv. Funct. Mater.* **2012**, *22*, 113–120. [CrossRef]
84. Akhtar, M.S.; Umar, A.; Ameen, S.; Imran, M.; Kumar, R.; Wang, Y.; Albargi, H.; Jalalah, M.; Alsaiari, M.A.; Ibrahim, A.A.; et al. Colloidal Synthesis of $NiMn_2O_4$nanodisks decorated reduced graphene oxide for electrochemical applications. *Microchem. J.* **2021**, *160*, 105630.
85. Zhu, Y.; Murali, S.; Cai, W.; Li, X.; Suk, J.W.; Potts, J.R.; Ruoff, R.S. Graphene and graphene oxide: Synthesis, properties, and applications. *Adv. Mater.* **2010**, *22*, 3906–3924. [CrossRef] [PubMed]
86. Liu, W.; Zeng, J.; Gao, Y.; Li, H.; de Rooij, N.; Umar, A.; Algarni, H.; Wang, Y.; Zhou, G. Charge transfer driven by redox dye molecules on graphene nanosheets for room-temperature gas sensing. *Nanoscale* **2021**, *13*, 18596–18607. [CrossRef] [PubMed]
87. Olean-Oliveira, A.; Oliveira Brito, G.A.; Cardoso, C.X.; Teixeira, M.F.S. Nanocomposite Materials Based on Electrochemically Synthesized Graphene Polymers: Molecular Architecture Strategies for Sensor Applications. *Chemosensors* **2021**, *9*, 149. [CrossRef]
88. Chen, Z.; Wang, J.; Cao, N.; Wang, Y.; Li, H.; de Rooij, N.F.; Umar, A.; Feng, Y.; French, P.J.; Zhou, G. Three-Dimensional Graphene-Based Foams with "Greater Electron Transferring Areas" Deriving High Gas Sensitivity. *ACS Appl. Nano Mater.* **2021**, *4*, 13234–13245. [CrossRef]

89. Wang, C.; Peng, Q.; Wu, J.; He, X.; Tong, L.; Luo, Q.; Li, J.; Moody, S.; Liu, H.; Wang, R.; et al. Mechanical characteristics of individual multi-layer graphene-oxide sheets under direct tensile loading. *Carbon* **2014**, *80*, 279–289. [CrossRef]
90. Pei, W.; Zhang, T.; Wang, Y.; Chen, Z.; Umar, A.; Li, H.; Guo, W. Enhancement of Charge Transfer between Graphene and Donor-π-Acceptor Molecule for Ultrahigh Sensing Performance. *Nanoscale* **2017**, *9*, 16273–16280. [CrossRef]
91. Zhang, J.; Li, P.; Zhang, Z.; Wang, X.; Tang, J.; Liu, H.; Shao, Q.; Ding, T.; Umar, A.; Guo, Z. Solvent-free graphene liquids: Promising candidates for lubricants without the base oil. *J. Colloid Interface Sci.* **2019**, *542*, 159–167. [CrossRef]
92. Chen, Z.; Wang, Y.; Shang, Y.; Umar, A.; Xie, P.; Qi, Q.; Zhou, G. One-Step Fabrication of Pyranine Modified- Reduced Graphene Oxide with Ultrafast and Ultrahigh Humidity Response. *Sci. Rep.* **2017**, *7*, 2713. [CrossRef] [PubMed]
93. Erickson, K.; Erni, R.; Lee, Z.; Alem, N.; Gannett, W.; Zettl, A. Determination of the local chemical structure of graphene oxide and reduced graphene oxide. *Adv. Mater.* **2010**, *22*, 4467–4472. [CrossRef] [PubMed]
94. Su, C.; Acik, M.; Takai, K.; Lu, J.; Hao, S.-J.; Zheng, Y.; Wu, P.; Bao, Q.; Enoki, T.; Chabal, Y.J. Probing the catalytic activity of porous graphene oxide and the origin of this behaviour. *Nat. Comm.* **2012**, *3*, 1298. [CrossRef]
95. Schafhaeutl, C. Ueber die Verbindungen des Kohlenstoffes Mit Silicium, Eisen und Andern Metallen, Welche die Verschiedenen Arten von Gusseisen, Stahl und Schmiedeeisen Bilden. *J. Prakt. Chem.* **1840**, *19*, 159–174. [CrossRef]
96. Brodie, B.C. On the atomic weight of graphite. *Philos. Trans. R. Soc. London* **1859**, *149*, 249–259.
97. Staudenmaier, L. Verfahrenzurdarstellung der graphits äure. *Ber. Dtsch. Chem. Ges.* **1898**, *31*, 1481–1487. [CrossRef]
98. Hummers Jr, W.S.; Offeman, R.E. Preparation of graphitic oxide. *J. Am. Chem. Soc.* **1958**, *80*, 1339. [CrossRef]
99. Fu, L.; Liu, H.B.; Zou, Y.; Li, B. Technology research on oxidative degree of graphite oxide prepared by Hummers method. *Carbon* **2005**, *124*, 10–14. (In Chinese)
100. Jeong, T.K.; Choi, M.K.; Sim, Y.; Lim, J.T.; Kim, G.S.; Seong, M.J.; Hyung, J.H.; Kim, K.S.; Umar, A.; Lee, S.K. Effect of graphene oxide ratio on the cell adhesion and growth behavior on a graphene oxide-coated silicon substrate. *Sci. Rep.* **2016**, *6*, 33835. [CrossRef]
101. Su, C.Y.; Xu, Y.; Zhang, W.; Zhao, J.; Tang, X.; Tsai, C.H.; Li, L.J. Electrical and spectroscopic characterizations of ultra-large reduced graphene oxide monolayers. *Chem. Mater.* **2009**, *21*, 5674–5680. [CrossRef]
102. Marcano, D.C.; Kosynkin, D.V.; Berlin, J.M.; Sinitskii, A.; Sun, Z.; Slesarev, A.; Alemany, L.B.; Lu, W.; Tour, J.M. Improved synthesis of graphene oxide. *ACS Nano* **2010**, *4*, 4806–4814. [CrossRef] [PubMed]
103. Sun, L.; Fugetsu, B. Mass production of graphene oxide from expanded graphite. *Mater. Lett.* **2013**, *109*, 207–210. [CrossRef]
104. Eigler, S.; Enzelberger-Heim, M.; Grimm, S.; Hofmann, P.; Kroener, W.; Geworski, A.; Dotzer, C.; Röckert, M.; Xiao, J.; Papp, C.; et al. Wet chemical synthesis of graphene. *Adv. Mater.* **2013**, *25*, 3583–3587. [CrossRef]
105. Chen, J.; Li, Y.; Huang, L.; Li, C.; Shi, G. High-yield preparation of graphene oxide from small graphite flakes via an improved Hummers method with a simple purification process. *Carbon* **2015**, *81*, 826–834. [CrossRef]
106. Panwar, V.; Chattree, A.; Pal, K. A new facile route for synthesizing of graphene oxide using mixture of sulfuric–nitric–phosphoric acids as intercalating agent. *Phys. E Low-Dimens. Syst. Nanostruct.* **2015**, *73*, 235–241. [CrossRef]
107. Peng, L.; Xu, Z.; Liu, Z.; Wei, Y.; Sun, H.; Li, Z.; Zhao, X.; Gao, C. An iron-based green approach to 1-hproduction of single-layer graphene oxide. *Nat. Commun.* **2015**, *6*, 5716. [CrossRef] [PubMed]
108. Rosillo-Lopez, M.; Salzmann, C.G. A simple and mild chemical oxidation route to high-purity nano-graphene oxide. *Carbon* **2016**, *106*, 56–63. [CrossRef]
109. Yu, H.; Zhang, B.; Bulin, C.; Li, R.; Xing, R. High-efficient synthesis of graphene oxide based on improved Hummers method. *Sci. Rep.* **2016**, *6*, 36143. [CrossRef]
110. Dimiev, A.M.; Ceriotti, G.; Metzger, A.; Kim, N.D.; Tour, J.M. Chemical mass production of graphene nanoplatelets in ~100% yield. *ACS Nano* **2016**, *10*, 274–279. [CrossRef]
111. Pei, S.; Wei, Q.; Huang, K.; Cheng, H.M.; Ren, W. Green synthesis of graphene oxide by seconds timescale water electrolytic oxidation. *Nat. Commun.* **2018**, *9*, 145. [CrossRef]
112. Ranjan, P.; Agrawal, S.; Sinha, A.; Rajagopala Rao, T.; Balakrishnan, J.; Thakur, A.D. A low-costnon-explosive synthesis of graphene oxide for scalable applications. *Sci. Rep.* **2018**, *8*, 12007. [CrossRef] [PubMed]
113. Hummers, J.W.S. Preparation of Graphitic Acid. U.S. Patent 2,798,878, 9 July 1957.
114. Becerril, H.A.; Mao, J.; Liu, Z.; Stoltenberg, R.M.; Bao, Z.; Chen, Y. Evaluation of solution-processed reduced GO films as transparent conductors. *ACS Nano* **2008**, *2*, 463–470. [CrossRef] [PubMed]
115. Li, D.; Mueller, M.B.; Gilje, S.; Kaner, R.B.; Wallace, G.G. Processable aqueous dispersions of graphene nanosheets. *Nat. Nanotechnol.* **2008**, *3*, 101–105. [CrossRef]
116. Abdolhosseinzadeh, S.; Asgharzadeh, H.; Kim, H.S. Fast and fully-scalable synthesis of reduced graphene oxide. *Sci. Rep.* **2015**, *5*, 10160. [CrossRef] [PubMed]
117. Chen, T.; Zeng, B.; Liu, J.; Dong, J.; Liu, X.; Wu, Z.; Yang, X.; Li, Z. High throughput exfoliation of graphene oxide from expanded graphite with assistance of strong oxidant in modified Hummers method. In *Journal of Physics: Conference Series*; IOP Publishing: Bristol, UK, 2009; p. 012051.
118. Hasani, A.; Dehsari, H.S.; Zarandi, A.A.; Salehi, A.; Taromi, F.A.; Kazeroni, H. Visible light-assisted photoreduction of graphene oxide using CdS nanoparticles and gas sensing properties. *J. Nanomater.* **2015**, *2015*, 71–82. [CrossRef]
119. Pan, X.; Ji, J.; Zhang, N.; Xing, M. Research progress of graphene-based nanomaterials for the environmental remediation. *Chin. Chem. Lett.* **2020**, *31*, 1462–1473. [CrossRef]

120. Zhang, M.; Okazaki, T.; Iizumi, Y.; Miyako, E.; Yuge, R.; Bandow, S.; Iijima, S.; Yudasaka, M. Preparation of small-sized graphene oxide sheets and their biological applications. *J. Mater. Chem. B* **2016**, *4*, 121–127. [CrossRef]
121. Hirata, M.; Gotou, T.; Horiuchi, S.; Fujiwara, M.; Ohba, M. Thin-film particles of graphite oxide 1: High-yield synthesis and flexibility of the particles. *Carbon* **2004**, *42*, 2929–2937. [CrossRef]
122. Kumar, P.V.; Bardhan, N.M.; Tongay, S.; Wu, J.; Belcher, A.M.; Grossman, J.C. Scalable enhancement of GO properties by thermally driven phase transformation. *Nat. Chem.* **2014**, *6*, 151–158. [CrossRef]
123. Chien, C.T.; Li, S.S.; Lai, W.J.; Yeh, Y.C.; Chen, H.A.; Chen, I.; Chen, L.C.; Chen, K.H.; Nemoto, T.; Isoda, S. Tunable photoluminescence from graphene oxide. *Angew. Chem. Int. Ed.* **2012**, *51*, 6662–6666. [CrossRef]
124. Luo, Z.; Vora, P.M.; Mele, E.J.; Johnson, A.C.; Kikkawa, J.M. Photoluminescence and band gap modulation in GO. *Appl. Phys. Lett.* **2009**, *94*, 111909. [CrossRef]
125. Liang, Y.; Wang, H.; Casalongue, H.S.; Chen, Z.; Dai, H. TiO2 nanocrystals grown on graphene as advanced photocatalytic hybrid materials. *Nano Res.* **2010**, *3*, 701–705. [CrossRef]
126. Wang, H.; Robinson, J.T.; Diankov, G.; Dai, H. Nanocrystal growth on graphene with various degrees of oxidation. *J. Am. Chem. Soc.* **2010**, *132*, 3270–3271. [CrossRef] [PubMed]
127. Chen, Z.; Wang, J.; Pan, D.; Wang, Y.; Noetzel, R.; Li, H.; Xie, P.; Pei, W.; Umar, A.; Jiang, L.; et al. Mimicking a Dog's Nose: Scrolling Graphene Nanosheets. *ACS Nano* **2018**, *12*, 2521–2530. [CrossRef]
128. Pitkethly, M.J. Nanomaterials-the driving force. *Mater. Today* **2004**, *7*, 20–29. [CrossRef]
129. Wu, Z.-S.; Ren, W.; Gao, L.; Liu, B.; Jiang, C.; Cheng, H.-M. Synthesis of high-quality graphene with a pre-determined number of layers. *Carbon* **2009**, *47*, 493–499. [CrossRef]
130. Johari, P.; Shenoy, V.B. Modulating optical properties of graphene oxide: Role of prominent functional groups. *ACS Nano* **2011**, *5*, 7640–7647. [CrossRef]
131. Kang, D.; Shin, H.S. Control of size and physical properties of graphene oxide by changing the oxidation temperature. *Carbon Lett.* **2012**, *13*, 39–43. [CrossRef]
132. Krishnamoorthy, K.; Veerapandian, M.; Yun, K.; Kim, S.-J. The chemical and structural analysis of GO with different degrees of oxidation. *Carbon* **2013**, *53*, 38–49. [CrossRef]
133. Bannov, A.; Timofeeva, A.; Shinkarev, V.; Dyukova, K.; Ukhina, A.; Maksimovskii, E.; Yusin, S. Synthesis and studies of properties of graphite oxide and thermally expanded graphite. *Prot. Metals. Phys. Chem. Surf.* **2014**, *50*, 183–190. [CrossRef]
134. Broughton, D.; Wentworth, R. Mechanism of decomposition of hydrogen peroxide solutions with manganese dioxide, I.J. *Am. Chem. Soc.* **1947**, *69*, 741–744. [CrossRef] [PubMed]
135. Hofmann, U.; Holst, R. Über die Säurenatur und die Methylierung von Graphitoxyd. *Ber. Dtsch. Chem. Ges. A B* **1939**, *72*, 754–771. [CrossRef]
136. Ruess, G. Ber das Graphitoxyhydroxyd (Graphitoxyd). *Mon. Fr. Chem.* **1947**, *76*, 381–417. [CrossRef]
137. Scholz, W.; Boehm, H.P. Untersuchungen am Graphitoxid. VI. Betrachtungen zur Struktur des Graphitoxids. *Z. Anorg. Allg. Chem.* **1969**, *369*, 327–340. [CrossRef]
138. Nakajima, T.; Matsuo, Y. Formation process and structure of graphite oxide. *Carbon* **1994**, *32*, 469–475. [CrossRef]
139. Lerf, A.; He, H.; Forster, M.; Klinowski, J. Structure of graphite oxide revisited II. *J. Phys. Chem. B* **1998**, *102*, 4477–4482. [CrossRef]
140. Savazzi, F.; Risplendi, F.; Mallia, G.; Harrison, N.M.; Cicero, G. Unravelling some of the structure–property relationships in graphene oxide at low degree of oxidation. *J. Phys. Chem. Lett.* **2018**, *9*, 1746–1749. [CrossRef] [PubMed]
141. Szabó, T.; Berkesi, O.; Forgó, P.; Josepovits, K.; Sanakis, Y.; Petridis, D.; Dékány, I. Evolution of surface functional groups in a series of progressively oxidized graphite oxides. *Chem. Mater.* **2006**, *18*, 2740–2749. [CrossRef]
142. Liu, Z.; Nørgaard, K.; Overgaard, M.H.; Ceccato, M.; Mackenzie, D.M.A.; Stenger, N.; Stipp, S.L.S.; Hassenkam, T. Direct observation of oxygen configuration on individual graphene oxide sheets. *Carbon* **2018**, *127*, 141–148. [CrossRef]
143. Chen, L.; Yu, H.; Zhong, J.; Song, L.; Wu, J.; Su, W. Graphene field emitters: A review of fabrication, characterization and properties. *Mater. Sci. Eng. B* **2017**, *220*, 44–58. [CrossRef]
144. Chen, X.; Fan, K.; Liu, Y.; Li, Y.; Liu, X.; Feng, W.; Wang, X. Recent advances in fluorinated graphene from synthesis to applications: Critical review on functional chemistry and structure engineering. *Adv. Mater.* **2022**, *34*, 2101665. [CrossRef] [PubMed]
145. Yin, P.T.; Shah, S.; Chhowalla, M.; Lee, K.B. Design, synthesis, and characterization of graphene–nanoparticle hybrid materials for bioapplications. *Chem. Rev.* **2015**, *115*, 2483–2531. [CrossRef]
146. Steinert, B.W.; Dean, D.R. Magnetic field alignment and electrical properties of solution cast PET–carbon nanotube composite films. *Polymer* **2009**, *50*, 898–904. [CrossRef]
147. Jia, R.; Xie, P.; Feng, Y.; Chen, Z.; Umar, A.; Wang, Y. Dipole-Modified Graphene with Ultrahigh Gas Sensibility. *Appl. Surface Sci.* **2018**, *440*, 409–414. [CrossRef]
148. Sun, Z.; Yan, Z.; Yao, J.; Beitler, E.; Zhu, Y.; Tour, J.M. Growth of graphene from solid carbon sources. *Nature* **2010**, *468*, 549–552. [CrossRef] [PubMed]
149. Shen, J.; Hu, Y.; Shi, M.; Lu, X.; Qin, C.; Li, C.; Ye, M. Fast and Facile Preparation of Graphene Oxide and Reduced Graphene Oxide Nanoplatelets. *Chem. Mater.* **2009**, *21*, 3514–3520. [CrossRef]
150. Stankovich, S.; Dikin, D.A.; Piner, R.D.; Kohlhaas, K.A.; Kleinhammes, A.; Jia, Y.; Wu, Y.; Nguyen, S.B.T.; Ruoff, R.S. Synthesis of Graphene-Based Nanosheets via Chemical Reduction of Exfoliated Graphite Oxide. *Carbon* **2007**, *45*, 1558–1565. [CrossRef]

151. Zhao, J.; Liu, L.; Li, F. Structural Characterization. In *Graphene Oxide: Physics and Applications*; Springer: Berlin/Heidelberg, Germany, 2015; pp. 15–29, Chapter 2.
152. Ganguly, A.; Sharma, S.; Papakonstantinou, P.; Hamilton, J. Probing the Thermal Deoxygenation of Graphene Oxide using High-Resolution in Situ X-ray-based Spectroscopies. *J. Phys. Chem. C* **2011**, *115*, 17009–17019. [CrossRef]
153. Hintermueller, D.; Prakash, R. Comprehensive Characterization of Solution-Cast Pristine and Reduced Graphene Oxide Composite Polyvinylidene Fluoride Films for Sensory Applications. *Polymers* **2022**, *14*, 2546. [CrossRef]
154. Ahmed, A.; Ibrahim, A.A.; Algadi, H.; Albargi, H.; Alsairi, M.A.; Wang, Y.; Akbar, S. Supramolecularly assembled isonicotinamide/ reduced graphene oxide nanocomposite for room-temperature NO_2 gas sensor. *Environ. Technol. Innov.* **2022**, *25*, 102066.
155. Bagri, A.; Mattevi, C.; Acik, M.; Chabal, Y.J.; Chhowalla, M.; Shenoy, V.B. Structural Evolution during the Reduction of Chemically Derived Graphene Oxide. *Nat. Chem.* **2010**, *2*, 581–587. [CrossRef] [PubMed]
156. Schniepp, H.C.; Li, J.-L.; McAllister, M.J.; Sai, H.; Herrera-Alonso, M.; Adamson, D.H.; Prud'homme, R.K.; Car, R.; Saville, D.A.; Aksay, I.A. Functionalized Single Graphene Sheets derived from Splitting Graphite Oxide. *J. Phys. Chem. B* **2006**, *110*, 8535–8539. [CrossRef] [PubMed]
157. Shahriary, L.; Athawale, A.A. Graphene Oxide Synthesized by using Modified Hummers Approach. *Int. J. Renew. Energy Environ. Eng.* **2014**, *2*, 58–63.
158. Wei, N.; Peng, X.; Xu, Z. Understanding Water Permeation in Graphene Oxide Membranes. *ACS Appl. Mater. Interfaces* **2014**, *6*, 5877–5883. [CrossRef]
159. Zhang, H.-B.; Zheng, W.G.; Yan, Q.; Yang, Y.; Wang, J.W.; Lu, Z.H.; Ji, G.Y.; Yu, Z.Z. Electrically conductive polyethylene terephthalate/graphene nanocomposites prepared by melt compounding. *Polymer* **2010**, *51*, 1191–1196. [CrossRef]
160. Seekaew, Y.; Lokavee, S.; Phokharatkul, D.; Wisitsoraat, A.; Kerdcharoen, T.; Wongchoosuk, C. Low-cost and flexible printed graphene–PEDOT: PSS gas sensor for ammonia detection. *Org. Electron.* **2014**, *15*, 2971–2981. [CrossRef]
161. Daoudi, K.; Gaidi, M.; Columbus, S.; Shameer, M.; Alawadhi, H. Hierarchically assembled silver nanoprism-graphene oxide-silicon nanowire arrays for ultrasensitive surface enhanced Raman spectroscopy sensing of atrazine. *Mater. Sci. Semicond. Processing* **2022**, *138*, 106288. [CrossRef]
162. Vandenabeele, P. ; *Practical Raman Spectroscopy: An introduction*; Wiley Online Library: Hoboken, NJ, USA, 2013.
163. Liu, W.-W.; Chai, S.P.; Mohamed, A.R.; Hashim, U. Synthesis and characterization of graphene and carbon nanotubes: A review on the past and recent developments. *Eng. Chem.* **2014**, *20*, 1171–1185. [CrossRef]
164. Gurunathan, S.; Arsalan Iqbal, M.; Qasim, M.; Park, C.H.; Yoo, H.; Hwang, J.H.; Uhm, S.J.; Song, H.; Park, C.; Do, J.T.; et al. Evaluation of Graphene Oxide Induced Cellular Toxicity and Transcriptome Analysis in Human Embryonic Kidney Cells. *Nanomaterials* **2019**, *9*, 969. [CrossRef]
165. Mantovani, S.; Khaliha, S.; Marforio, T.D.; Kovtun, A.; Favaretto, L.; Tunioli, F.; Bianchi, A.; Petrone, G.; Liscio, A.; Palermo, V.; et al. Facile high-yield synthesis and purification of lysine-modified graphene oxide for enhanced drinking water purification. *Chem. Commun.* **2022**, *58*, 9766–9769. [CrossRef]
166. Lan, Q.; Liu, L.; Wu, Y.; Feng, C.; Ou, K.; Wang, Z.; Huang, Y.; Lv, Y.; Miao, Y.E.; Liu, T. Porous reduced graphene oxide/phenolic nanomesh membranes with ternary channels for ultrafast water purification. *Compos. Commun.* **2022**, *33*, 101216. [CrossRef]
167. Park, S.; Lee, K.S.; Bozoklu, G.; Cai, W.; Nguyen, S.T.; Ruoff, R.S. Graphene oxide papers modified by divalent ions—Enhancing mechanical properties via chemical cross-linking. *ACS Nano* **2008**, *2*, 572–578. [CrossRef]
168. Chen, D.; Feng, H.; Li, J. Graphene oxide: Preparation, functionalization, and electrochemical applications. *Chem. Rev.* **2012**, *112*, 6027–6053. [CrossRef] [PubMed]
169. Hamad, H.N.; Idrus, S. Recent Developments in the Application of Bio-Waste-Derived Adsorbents for the Removal of Methylene Blue from Wastewater: A Review. *Polymers* **2022**, *14*, 783. [CrossRef] [PubMed]
170. Dreyer, D.R.; Todd, A.D.; Bielawski, C.W. Harnessing the chemistry of graphene oxide. *Chem. Soc. Rev.* **2014**, *43*, 5288–5301. [CrossRef]
171. Gao, Y.; Wang, J.; Feng, Y.; Cao, N.; Li, H.; de Rooij, N.; Umar, A.; French, P.J.; Wang, Y.; Zhou, G. Carbon-Iron Electron Transport Channels in Porphyrin–Graphene Complex for ppb-Level Room-Temperature NO Gas Sensing. *Small* **2022**, *18*, 2103259. [CrossRef]
172. Singh, R.K.; Kumar, R.; Singh, D.P. Graphene oxide: Strategies for synthesis, reduction and frontier applications. *RSC Adv.* **2016**, *6*, 64993–65011. [CrossRef]
173. Wang, Y.; Wu, Y.; Huang, Y.; Zhang, F.; Yang, X.; Ma, Y.; Chen, Y. Preventing graphene sheets from restacking for high-capacitance performance. *J. Phys. Chem. C* **2011**, *115*, 23192–23197. [CrossRef]
174. Chen, Z.; Wang, J.; Umar, A.; Wang, Y.; Li, H.; Zhou, G. Three-Dimensional Crumpled Graphene-Based Nanosheets with Ultrahigh NO_2 Gas Sensibility. *ACS Appl. Mater. Interfaces* **2017**, *9*, 11819–11827. [CrossRef]
175. Bao, Q.; Zhang, D.; Qi, P. Synthesis and characterization of silver nanoparticle and graphene oxide nanosheet composites as a bactericidal agent for water disinfection. *J. Colloid Interface Sci.* **2011**, *360*, 463–470. [CrossRef]
176. Chaitoglou, S.; Zisis, G.; Spachis, L.; Raptis, I.; Papanikolaou, N.; Vavouliotis, A.; Penedo, R.; Fernandes, N.; Dimoulas, A. Layer-by-layer assembled graphene coatings on polyurethane films as He permeation barrier. *Prog. Org. Coat.* **2021**, *150*, 105984. [CrossRef]

177. Sun, X.-F.; Qin, J.; Xia, P.-F.; Guo, B.-B.; Yang, C.-M.; Song, C.; Wang, S.G. Graphene oxide–silver nanoparticle membrane for biofouling control and water purification. *Chem. Eng. J.* **2015**, *281*, 53–59. [CrossRef]
178. Goyat, R.; Singh, J.; Umar, A.; Saharan, Y.; Kumar, V.; Algadi, H.; Akbar, S.; Baskoutas, S. Modified low-temperature synthesis of graphene oxide nanosheets: Enhanced adsorption, antibacterial and antioxidant properties. *Environ. Res.* **2022**, *215*, 114245. [CrossRef] [PubMed]
179. Wu, H.; Tang, B.; Wu, P. Development of novel SiO2-GO nanohybrid/polysulfone membrane with enhanced performance. *J. Memb. Sci.* **2014**, *451*, 94–102. [CrossRef]
180. Safarpour, M.; Vatanpour, V.; Khataee, A. Preparation and characterization of graphene oxide/TiO_2 blended PES nanofiltration membrane with improved antifouling and separation performance. *Desalination* **2015**, *393*, 65–78. [CrossRef]
181. Xiao, Y.; Liu, J.; Lin, Y.; Lin, W.; Fang, Y. Novel graphene oxide-silver nanorod composites with enhanced photocatalytic performance under visible light irradiation. *J. Alloys Compd.* **2017**, *698*, 170–177. [CrossRef]
182. La, D.D.; Patwari, J.M.; Jones, L.A.; Antolasic, F.; Bhosale, S.V. Fabrication of a GNP/Fe–Mg binary oxide composite for effective removal of arsenic from aqueous solution. *ACS Omega* **2017**, *2*, 218–226. [CrossRef]
183. Jiao, T.; Liu, Y.; Wu, Y.; Zhang, Q.; Yan, X.; Gao, F.; Bauer, A.J.P.; Liu, J.; Zeng, T.; Li, B. Facile and scalable preparation of graphene oxide-based magnetic hybrids for fast and highly efficient removal of organic dyes. *Sci. Rep.* **2015**, *5*, 12451. [CrossRef]
184. Kumar, S.; Nair, R.R.; Pillai, P.B.; Gupta, S.N.; Iyengar, M.A.R.; Sood, A.K. Graphene oxide–$MnFe_2O_4$ magnetic nanohybrids for efficient removal of lead and arsenic from water. *ACS Appl. Mater. Interfaces* **2014**, *6*, 17426–17436. [CrossRef]
185. Luo, X.; Wang, C.; Wang, L.; Deng, F.; Luo, S.; Tu, X.; Au, C. Nanocomposites of graphene oxide-hydrated zirconium oxide for simultaneous removal of As(III) and As(V) from water. *Chem. Eng. J.* **2013**, *220*, 98–106. [CrossRef]
186. Yang, X.; Chen, C.; Li, J.; Zhao, G.; Ren, X.; Wang, X. Graphene oxide-iron oxide and reduced graphene oxide iron oxide hybrid materials for the removal of organic and inorganic pollutants. *RSC Adv.* **2012**, *2*, 8821–8826. [CrossRef]
187. Lee, Y.-C.; Yang, J.-W. Self-assembled flower-like TiO2 on exfoliated graphite oxide for heavy metal removal. *J. Ind. Eng. Chem.* **2012**, *18*, 1178–1185. [CrossRef]
188. Beura, R.; Thangadurai, P. Structural, optical and photocatalytic properties of graphene-ZnO nanocomposites for varied compositions. *J. Phys. Chem. Solids* **2017**, *102*, 168–177. [CrossRef]
189. Anirudhan, T.S.; Deepa, J.R. Nano-zinc oxide incorporated graphene oxide/nanocellulose composite for the adsorption and photo catalytic degradation of ciprofloxacin hydrochloride from aqueous solutions. *J. Colloid Interface Sci.* **2017**, *490*, 343–356. [CrossRef]
190. Shan, X.; Guo, X.; Yin, Y.; Miao, Y.; Dong, H. Surface modification of graphene oxide by goethite with enhanced tylosin photocatalytic activity under visible light irradiation. *Colloids Surf. A Physicochem. Eng. Asp.* **2017**, *520*, 420–427. [CrossRef]
191. Huang, T.; Wu, J.; Zhao, Z.; Zeng, T.; Zhang, J.; Xu, A.; Zhou, X.; Qi, Y.; Ren, J.; Zhou, R.; et al. Synthesis and photocatalytic performance of CuO-CeO2/graphene oxide. *Mater. Lett.* **2016**, *185*, 503–506. [CrossRef]
192. Castro-Muñoz, R.; Yáñez-Fernández, J.; Fíla, V. Phenolic compounds recovered from agro-food by-products using membrane technologies: An overview. *Food Chem.* **2016**, *213*, 753–762. [CrossRef]
193. Van der Bruggen, B.; Curcio, E.; Drioli, E. Process intensification in the textile industry: The role of membrane technology. *J. Environ. Manag.* **2004**, *73*, 267–274. [CrossRef]
194. Saharan, Y.; Singh, J.; Goyat, R.; Umar, A.; Algadi, H.; Ibrahim, A.A.; Kumar, R.; Baskoutas, S. Nanoporous and hydrophobic new Chitosan-Silica blend aerogels for enhanced oil adsorption capacity. *J. Clean. Prod.* **2022**, *351*, 131247. [CrossRef]
195. Castro-Muñoz, R.; Barragán-Huerta, B.E.; Fíla, V.; Denis, P.C.; Ruby-Figueroa, R. Current Role of Membrane Technology: From the Treatment of Agro-Industrial by-Products up to the Valorization of Valuable Compounds. *Waste Biomass Valorization* **2018**, *9*, 513–529. [CrossRef]
196. Roy, S.; Singha, N.R. Polymeric Nanocomposite Membranes for Next Generation Pervaporation Process: Strategies, Challenges and Future Prospects. *Membranes* **2017**, *7*, 53. [CrossRef] [PubMed]
197. Zhong, D.; Zhang, J.; Lv, L.; Lv, Y.; Jiang, Y. Magnetically Ultrastabilized Graphene Oxide-Based Membrane Filter for Point-of-Use Water Treatment. *ACS EST Eng.* **2022**, *2*, 769–779. [CrossRef]
198. Al-Gamal, A.Q.; Saleh, T.A. Design and manufacturing of a novel thin-film composite membrane based on polyamidoamine-grafted graphene nanosheets for water treatment. *J. Water Process Eng.* **2022**, *47*, 102770. [CrossRef]
199. Jia, F.; Xiao, X.; Nashalian, A.; Shen, S.; Yang, L.; Han, Z.; Qu, H.; Wang, T.; Ye, Z.; Zhu, Z.; et al. Advances in graphene oxide membranes for water treatment. *Nano Res.* **2022**, *15*, 6636–6654. [CrossRef]
200. Raza, A.; Hassan, J.Z.; Mahmood, A.; Nabgan, W.; Ikram, M. Recent advances in membrane-enabled water desalination by 2D frameworks: Graphene and beyond. *Desalination* **2022**, *531*, 115684. [CrossRef]
201. Kumar, M.; Sreedhar, N.; Thomas, N.; Mavukkandy, M.; Ismail, R.A.; Aminabhavi, T.M.; Arafat, H.A. Polydopamine-coated graphene oxide nanosheets embedded in sulfonated poly (ether sulfone) hybrid UF membranes with superior antifouling properties for water treatment. *Chem. Eng. J.* **2022**, *433*, 133526. [CrossRef]
202. Lalia, B.S.; Kochkodan, V.; Hashaikeh, R.; Hilal, N. A review on membrane fabrication: Structure, properties and performance relationship. *Desalination* **2013**, *326*, 77–95. [CrossRef]
203. Kim, J.; van der Bruggen, B. The use of nanoparticles in polymeric and ceramic membrane structures: Review of manufacturing procedures and performance improvement for water treatment. *Environ. Pollut.* **2010**, *158*, 2335–2349. [CrossRef]

204. Ng, L.Y.; Mohammad, A.W.; Leo, C.P.; Hilal, N. Polymeric membranes incorporated with metal/metal oxide nanoparticles: A comprehensive review. *Desalination* **2013**, *308*, 15–33. [CrossRef]
205. Kim, E.B.; Imran, M.; Umar, A.; Akhtar, M.S.; Ameen, S. Indandione oligomer @graphene oxide functionalized nanocomposites for enhanced and selective detection of trace Cr^{2+} and Cu^{2+} ions. *Adv. Compos. Hybrid Mater.* **2022**, *5*, 1582–1594. [CrossRef]
206. Al Aani, S.; Wright, C.J.; Atieh, M.A.; Hilal, N. Engineering nanocomposite membranes: Addressing current challenges and future opportunities. *Desalination* **2017**, *401*, 1–15. [CrossRef]
207. Mueller, N.C.; van der Bruggen, B.; Keuter, V.; Luis, P.; Melin, T.; Pronk, W.; Reisewitz, R.; Rickerby, D.; Rios, G.M.; Wennekes, W.; et al. Nanofiltration and nanostructured membranes-Should they be considered nanotechnology or not? *J. Hazard. Mater.* **2012**, *211–212*, 275–280. [CrossRef] [PubMed]
208. Marino, A.F.T.; Boerrigter, M.; Faccini, M.; Chaumette, C.; Arockiasamy, L.; Bundschuh, J. Photocatalytic activity and synthesis procedures of TiO_2 nanoparticles for potential applications in membranes. In *Application of Nanotechnology in Membranes for Water Treatment*; Figoli, J.B.A., Hoinkis, J., Altinkaya, S.A., Eds.; CRC Press: Boca Raton, FL, USA; Taylor & Francis Group: Abingdon, UK, 2017.
209. Cheng, M.; Yao, C.; Su, Y.; Liu, J.; Xu, L.; Bu, J.; Wang, H.; Hou, S. Cyclodextrin modified graphene membrane for highly selective adsorption of organic dyes and copper (II) ions. *Eng. Sci.* **2022**, *18*, 299–307. [CrossRef]
210. Meshhal, M.; Kühn, O. Diffusion of Water Confined between Graphene Oxide Layers: Implications for Membrane Filtration. *ACS Appl. Nano Mater.* **2022**, *5*, 11119–11128. [CrossRef]
211. Liu, T.; Lyv, J.; Xu, Y.; Zheng, C.; Liu, Y.; Fu, R.; Liang, L.; Wu, J.; Zhang, Z. Graphene-based woven filter membrane with excellent strength and efficiency for water desalination. *Desalination* **2022**, *533*, 115775. [CrossRef]
212. Kumar, M.; Mukherjee, T.K.; Sharma, I.; Upadhyay, S.K.; Singh, R. Role of Bacteria in Bioremediation of Chromium from Wastewaters: An Overview. *Bio Sci. Res. Bull.* **2021**, *37*, 77–87. [CrossRef]
213. Xu, K.; Ding, P.; Li, Y.; Chen, L.; Xu, J.; Duan, X.; Zeng, F. Graphene Directly Growth on Non-Metal Substrate from Amorphous Carbon Nano Films Without Transfer and Its Application in Photodetector. *Sci. Adv. Mater.* **2021**, *13*, 574–582. [CrossRef]
214. Celik, E.; Park, H.; Choi, H.; Choi, H. Carbon nanotube blended polyethersulfone membranes for fouling control in water treatment. *Water Res.* **2011**, *45*, 274–282. [CrossRef]
215. Xia, S.; Ni, M. Preparation of poly (vinylidene fl uoride) membranes with graphene oxide addition for natural organic matter removal. *J. Membr. Sci.* **2015**, *473*, 54–62. [CrossRef]
216. Arsuaga, J.M.; Sotto, A.; del Rosario, G.; Martínez, A.; Molina, S.; Teli, S.B.; de Abajo, J. Influence of the type, size, and distribution of metal oxide particles on the properties of nanocomposite ultrafiltration membranes. *J. Membr. Sci.* **2013**, *428*, 131–141. [CrossRef]
217. Liang, S.; Xiao, K.; Mo, Y.; Huang, X. A novel ZnO nanoparticle blended polyvinylidene fluoride membrane for anti-irreversible fouling. *J. Membr. Sci.* **2012**, *394–395*, 184–192. [CrossRef]
218. Zhang, X.; Wang, Y.; Liu, Y.; Xu, J.; Han, Y.; Xu, X. Preparation, performances of PVDF/ZnO hybrid membranes and their applications in the removal of copper ions. *Appl. Surf. Sci.* **2014**, *316*, 333–340. [CrossRef]
219. Hong, J.; He, Y. Effects of nano sized zinc oxide on the performance of PVDF micro filtration membranes. *Desalination* **2012**, *302*, 71–79. [CrossRef]
220. Ahmad, A.L.; Abdulkarim, A.A.; Ismail, S.; Seng, O.B. Optimization of PES/ZnO mixed matrix membrane preparation using response surface methodology for humic acid removal. *Korean J. Chem. Eng.* **2016**, *33*, 997–1007. [CrossRef]
221. Chung, Y.T.; Ba-abbad, M.M.; Mohammad, A.W. Functionalization of zinc oxide (ZnO) nanoparticles and its effects on polysulfone-ZnO membranes. *Desalin. Water Treat.* **2017**, *57*, 7801–7811. [CrossRef]
222. Ghoul, J.E.L.; Ghiloufi, I.; Mir, L.E.L.; Arabia, S. Efficiency of polyamide thin-film nanocomposite membrane containing ZnO nanoparticles. *J. Ovonic Res.* **2017**, *13*, 83–90.
223. Engineering, M.; Jia, H.; Wu, Z.; Liu, N. Effect of nano-ZnO with different particle size on the performance of PVDF composite membrane. *Plast. Rubber Compos.* **2016**, *46*, 1–7.
224. Dipheko, T.D.; Matabola, K.P.; Kotlhao, K.; Moutloali, R.M.; Klink, M. Fabrication and Assessment of ZnO Modified Polyethersulfone Membranes for Fouling Reduction of Bovine Serum Albumin. *Int. J. Polym. Sci.* **2017**, *2017*, 3587019. [CrossRef]
225. Jo, Y.J.; Choi, E.Y.; Choi, N.W.; Kim, C.K. Antibacterial and Hydrophilic Characteristics of Poly (ether sulfone) Composite Membranes Containing Zinc Oxide Nanoparticles Grafted with Hydrophilic Polymers. *Ind. Eng. Chem. Res.* **2016**, *55*, 7801–7809. [CrossRef]
226. Zhao, S.; Yan, W.; Shi, M.; Wang, Z.; Wang, J. Improving permeability and antifouling performance of polyethersulfone ultra fi ltration membrane by incorporation of ZnO-DMF dispersion containing nano-ZnO and polyvinylpyrrolidone. *J. Membr. Sci.* **2015**, *478*, 105–116. [CrossRef]
227. Bai, H.; Liu, Z.; Sun, D.D. A hierarchically structured and multifunctional membrane for water treatment. *Appl. Catal. B Environ.* **2012**, *111–112*, 571–577. [CrossRef]
228. Bahadar, S.; Alamry, K.A.; Bifari, E.N.; Asiri, A.M.; Yasir, M.; Gzara, L.; Zulfiqar, R. Assessment of antibacterial cellulose nanocomposites for water permeability and salt rejection. *J. Ind. Eng. Chem.* **2015**, *24*, 266–275.
229. Akin, I.; Ersoz, M. Preparation and characterization of CTA/m-ZnO composite membrane for transport of Rhodamine B. *Desalin. Water Treat.* **2016**, *57*, 3037–3047. [CrossRef]

230. Li, H.; Shi, W.; Zhu, H.; Zhang, Y.; Du, Q.; Qin, X. Effects of Zinc Oxide Nanospheres on the Separation Performance of Hollow Fiber Poly (piperazine-amide) Composite Nanofiltration Membranes. *Fibers Polym.* **2016**, *17*, 836–846. [CrossRef]
231. Zhao, X.; Li, J.; Liu, C. Improving the separation performance of the forward osmosis membrane based on the etched microstructure of the supporting layer. *Desalination* **2017**, *408*, 102–109. [CrossRef]
232. Isawi, H.; El-sayed, M.H.; Feng, X.; Shawky, H.; Abdel, M.S. Applied Surface Science Surface nanostructuring of thin film composite membranes via grafting polymerization and incorporation of ZnO nanoparticles. *Appl. Surf. Sci.* **2016**, *385*, 268–281. [CrossRef]
233. Badrinezhad, L.; Ghasemi, S. Preparation and characterization of polysulfone/graphene oxide nanocomposite membranes for the separation of methylene blue from water. *Polym. Bull.* **2017**, *75*, 469–484. [CrossRef]
234. Zhao, C.; Xu, X.; Chen, J.; Yang, F. Optimization of preparation conditions of poly (vinylidene fluoride)/graphene oxide micro fi ltration membranes by the Taguchi experimental design. *Desalination* **2014**, *334*, 17–22. [CrossRef]
235. Morales-Torres, S.; Pastrana-Martı, L.M.; Figueiredo, L.; Faria, J.L.; Silva, A.M.T. Graphene oxide based ultrafiltration membranes for photocatalytic degradation of organic pollutants in salty water. *Water Res.* **2015**, *7*, 179–190.
236. Kiran, S.A.; Thuyavan, Y.L.; Arthanareeswaran, G.; Matsuura, T.; Ismail, A.F. Impact of graphene oxide embedded polyethersulfone membranes for the effective treatment of distillery effluent. *Chem. Eng. J.* **2016**, *286*, 528–537. [CrossRef]
237. Zinadini, S.; Akbar, A.; Rahimi, M.; Vatanpour, V. Preparation of a novel antifouling mixed matrix PES membrane by embedding graphene oxide nanoplates. *J. Membr. Sci.* **2014**, *453*, 292–301. [CrossRef]
238. Chae, H.; Lee, J.; Lee, C.; Kim, I.; Park, P. Graphene oxide-embedded thin-film composite reverse osmosis membrane with high flux, anti-biofouling, and chlorine resistance. *J. Membr. Sci.* **2015**, *483*, 128–135. [CrossRef]
239. Ali, M.E.A.; Wang, L.; Wang, X.; Feng, X. Thin film composite membranes embedded with graphene oxide for water desalination. *Desalination* **2016**, *386*, 67–76. [CrossRef]
240. Shen, L.; Xiong, S.; Wang, Y. Graphene oxide incorporated thin- fi lm composite membranes for forward osmosis applications. *Chem. Eng. Sci.* **2016**, *143*, 194–205. [CrossRef]
241. Crock, C.A.; Rogensues, A.R.; Shan, W.; Tarabara, V.V. Polymer nanocomposites with graphene-based hierarchical fillers as materials for multifunctional water treatment membranes. *Water Res.* **2013**, *47*, 3984–3996. [CrossRef] [PubMed]
242. Han, Y.; Xu, Z.; Gao, C. Ultrathin Graphene Nanofi ltration Membrane forWater Purification. *Adv. Funct. Mater.* **2013**, *23*, 3693–3700. [CrossRef]
243. Toroghi, M.; Raisi, A.; Aroujalian, A. Preparation and characterization of polyethersulfone/silver nanocomposite ultrafiltration membrane for antibacterial applications. *Polym. Adv. Technol.* **2014**, *25*, 711–722. [CrossRef]
244. Zhang, M.; Zhang, K.; de Gusseme, B.; Verstraete, W. Biogenic silver nanoparticles (bio-Ag0) decrease biofouling of bio-Ag0/PES nanocomposite membranes. *Water Res.* **2012**, *46*, 2077–2087. [CrossRef]
245. Koseoglu-Imer, D.Y.; Kose, B.; Altinbas, M.; Koyuncu, I. The production of polysulfone (PS) membrane with silver nanoparticles (AgNP): Physical properties, filtration performances, and biofouling resistances of membranes. *J. Membr. Sci.* **2013**, *428*, 620–628. [CrossRef]
246. Ben-Sasson, M.; Lu, X.; Bar-Zeev, E.; Zodrow, K.R.; Nejati, S.; Qi, G.; Giannelis, E.P.; Elimelech, M. In situ formation of silver nanoparticles on thin-film composite reverse osmosis membranes for biofouling mitigation. *Water Res.* **2014**, *62*, 260–270. [CrossRef]
247. Yang, Z.; Wu, Y.; Wang, J.; Cao, B.; Tang, C.Y. In situ reduction of silver by polydopamine: A novel antimicrobial modification of a thin-film composite polyamide membrane. *Environ. Sci. Technol.* **2016**, *50*, 9543–9550. [CrossRef] [PubMed]
248. Hoek, E.M.V.; Ghosh, A.K.; Huang, X.; Liong, M.; Zink, J.I. Physical-chemical properties, separation performance, and fouling resistance of mixed-matrix ultrafiltration membranes. *Desalination* **2011**, *283*, 89–99. [CrossRef]
249. Shi, F.; Ma, Y.; Ma, J.; Wang, P.; Sun, W. Preparation and characterization of PVDF/TiO_2 hybrid membranes with different dosage of nano-TiO_2. *J. Membr. Sci.* **2012**, *389*, 522–531. [CrossRef]
250. Amini, M.; Rahimpour, A.; Jahanshahi, M. Forward osmosis application of modified TiO_2-polyamide thin film nanocomposite membranes. *Desalin. Water Treat.* **2016**, *57*, 14013–14023. [CrossRef]
251. Emadzadeh, D.; Lau, W.J.; Matsuura, T.; Rahbari-Sisakht, M.; Ismail, A.F. A novel thin film composite forward osmosis membrane prepared from PSf-TiO_2 nanocomposite substrate for water desalination. *Chem. Eng. J.* **2014**, *237*, 70–80. [CrossRef]